Submitted to Advances in Quantum Electronics

RECEIVED
LAWRENCE
RADIATION LABORATORY

MAY 22 1974

LIBRARY AND
DOCUMENTS SECTION

LBL-2703
Preprint

SELF-FOCUSING OF LIGHT: REVIEW ON EXPERIMENTAL RESULTS AND PHYSICAL INTERPRETATIONS

Y. R. Shen

March 1974

Prepared for the U. S. Atomic Energy Commission
under Contract W-7405-ENG-48

TWO-WEEK LOAN COPY

This is a Library Circulating Copy which may be borrowed for two weeks. For a personal retention copy, call Tech. Info. Division, Ext. 5545

LAWRENCE BERKELEY LABORATORY
UNIVERSITY OF CALIFORNIA
BERKELEY

LBL-2703

DISCLAIMER

This document was prepared as an account of work sponsored by the United States Government. While this document is believed to contain correct information, neither the United States Government nor any agency thereof, nor the Regents of the University of California, nor any of their employees, makes any warranty, express or implied, or assumes any legal responsibility for the accuracy, completeness, or usefulness of any information, apparatus, product, or process disclosed, or represents that its use would not infringe privately owned rights. Reference herein to any specific commercial product, process, or service by its trade name, trademark, manufacturer, or otherwise, does not necessarily constitute or imply its endorsement, recommendation, or favoring by the United States Government or any agency thereof, or the Regents of the University of California. The views and opinions of authors expressed herein do not necessarily state or reflect those of the United States Government or any agency thereof or the Regents of the University of California.

Self-Focusing of Light: Review on Experimental Results and Physical Interpretations

Y. R. Shen

Department of Physics, University of California
and
Inorganic Materials Research Division,
Lawrence Berkeley Laboratory,
Berkeley, California 94720

I. Introduction.

Self-focusing of light in a nonlinear medium has been one of the most interesting subjects in nonlinear optics. Over the last ten years, it has fascinated a large number of research workers. Although it is just one of the nonlinear wave propagation problems, many unexpected but extremely interesting phenomena have come out of it. The formalism of the problem looks simple, but to solve it rigorously requires the biggest computer in the world. Appropriate approximations must be used in the process of solving the problem. Great physical insight and ingenuity are needed in making these approximations. In fact, this is where interesting physics comes in. The problem is like a jig-saw puzzle. The pieces are being put together through slow steps of closely coupled theoretical and experimental advances.

Self-focusing is a fundamental problem, but it is also important for practical applications. It is often responsible for the optical damages created in a solid by a high-power laser beam. It is also sometimes responsible for the poor characteristics of a laser beam. In fact, self-focusing is presently the limiting factor in the design of high-power laser amplifiers. Self-focusing can also have strong influence on other physical processes in a medium. It may play an important role in generating plasmas through optical breakdown.

In the process of studying self-focusing over the years, a number of controversies arose. Most of these controversies have now been resolved, but unfortunately some argument, mainly on questions of semantics, still exists among various research workers. In this paper, we wish to clear up such a confusion.

We shall use the following terms to describe the various different physical pictures and processes. A "focus" is not necessarily a sharp point but can extend over a large region. A "filament" simply means an intense streak of light parallel to the direction of beam propagation with no further implication. "Self-focusing" describes in general focusing of the beam by itself as a result of the nonlinear refractive index induced by the beam. "Self-trapping" describes the trapping of light in a dielectric channel created by the instantaneous response of the nonlinear refractive index to the light beam.[1] "Trapping" simply means the trapping of light in a dielectric channel without referring to any specific mechanism responsible for trapping. "Dynamic trapping" describes the momentary trapping of a trailing portion of the light pulse in a dielectric channel induced by the leading portion of the pulse.

The outline of the paper is as follows. In Sec. II, we review the historical development of the subject. In Sec. III, we give a basic physical description of the self-focusing phenomenon. In Secs. IV and V, we discuss the experimental results and the corresponding physical interpretations on quasi-steady-state self-focusing of a nanosecond pulse in ordinary Kerr liquids and transient self-focusing in solids respectively. In Sec. VI, we discuss transient self-focusing in

Kerr liquids, mainly with a picosecond pulse.

Finally, in Sec. VII, we consider self-focusing in gases and thermal self-focusing in solids briefly.

The reference list in this paper certainly does not cover all the published work on this subject. The readers will find more references on theoretical calculations in the following article by Marburger. They are also urged to consult the article by Kerr for more complete references up to 1970 and the recent review papers by Akhmanov et al [3] and by Svelto for references up to the summer of 1972.[4] The author would like to appologize for the possible omission in this paper of some important work on this subject.

II. Historical Development

While the most important application of self-focusing at present is on how to avoid self-focusing which would lead to optical breakdown, it was in fact the study of optical damage in solids which initiated the investigation of self-focusing. In early 1964, Hercher [5] found that by focusing unto a solid a Q-switched laser beam of more than a few megawatts, one would obtain long threads of damage spots with a diameter of few microns. In order to explain the observed phenomenon, Chiao, Garmire, and Townes [1] proposed the self-trapping model. They showed that in materials with a positive field-induced refractive index, a light beam can produce its own dielectric waveguide and propagate without any change in the beam profile. Presumably, the damage tracks were induced by the intense self-trapped beam. However, they did not analyze the

dynamics in creating and maintaining such a self-trapped beam. Askar'yan[6] in fact first suggested the possibility of observing the effects of nonlinear refractive index on beam propagation. Talanov[7] found independently the self-trapping solution for a beam in a nonlinear medium.

In the meantime, stimulated Raman scattering in both liquids and solids was observed.[8] In most cases, one found anomalous effects: namely, the stimulated scattering had a very sharp threshold, an unreasonably high gain, a forward-backward gain asymmetry,[8] and anomalous anti-Stokes rings which could not be explained by any theory of stimulated raman scattering.[10] It was soon realized that these anomalies were due to self-focusing of the laser beam in the medium.[11-13] Talanov[12] and Kelley[13] showed that in the self-focusing process, the beam shrinks rather suddenly to a very small size at a distance known as the self-focusing distance, and the beam intensity increases correspondingly as the beam diameter decreases. The sudden increase of the beam intensity in self-focusing accounts qualitatively for the observed anomalies in the stimulated Raman scattering.

Using the sharp onset of stimulated Raman scattering as an indication of self-focusing, Wang[14] was then able to verify quantitatively Kelley's prediciton on the self-focusing distance. Garmire, Chiao, and Townes[15] preferred to look at the self-focused beam directly. They managed to photograph simultaneously the beam profiles at various points in CS_2 by inserting a set of milar films as beam splitters in the liquid cell. They found that the

beam did in fact shrink suddenly into a "filament" of about 100 μm in diameter at approximately the self-focusing distance predicted by Kelley.[13] The observed "filament" seemed to be due to self-trapping suggested earlier by the same group.[1] However, the photographic system used in this experiment was of poor resolution. Later, with a better resolution, Chiao et al.[16] showed that within this 100 μm "filament", there were actually around 100 "small-scale filaments" of only few microns in diameter. (See Fig.1) The characteristics of these small "filaments" were measured[16-19] and the self-trapping model was used to interpret the results.[16-19]

This multi-filament picture was rather surprising and interesting, and had stimulated a lot of thinking. For example, it was suggested that these filaments could be an analog to the quantized flux lines in a type - II superconductor.[20] However, we learned later that when a single-mode laser was used in the self-focusing experiment, only one single "filament" could be observed as one would expect.[21] (Fig. 2)

The self-focusing calculations of Talanov,[12] Kelley,[13] and others[22] all diverge at the focal spot, and therefore is valid only in the prefocal region where the beam diameter is still relatively large. Results from such calculations have been

verified quantitatively in experiments with single-mode lasers by McAllister et al.[23] and by Maier et al.[24] Subsequent to the earlier calculations,[12,13,22] a large number of theoretical papers were published, discussing the many possible aspects of self-focusing.[25] Goldberg et al.[26] and Marburger and Dawes[27] modified and extended the numerical calculation of Kelley.[13] They carried the calculation through the focal region by assuming a saturable nonlinear refractive index. Unfortunately, the assumption was not physically reasonable for liquids and solids. How an incoming beam could self-focus into one or many self-trapped filaments remained a mystery. In fact, it can be shown that the self-trapping solution is an unstable one. Any small perturbation would make the self-trapped beam either diffract or self-focus. It may be possible that the self-trapped beam can be stabilized when higher-order nonlinearities or other nonlinear effects are included, but no such solution has ever been obtained. It is also not very likely that a sharply self-focused beam would tunnel into a self-trapped filament since energetically it is an unfavourable situation. Then, the question often raised was: "How would you explain the observed 'filaments' if they were not the self-trapped filaments ?"

In all the earlier calculations, the laser power was assumed to be time-independent. However, in the experiments, pulsed lasers were always used. Marburger and Wagner[28] first pointed out that with time-varying laser power, the focal region of self-focusing would move in time. Lugovoi et al.[29] suggested that the moving focal spots resulting from self-focusing of a laser pulse would

produce streaks of light and could perhaps explain the observed "filaments". By using the result of the quasi-steady-state approximation for a single-mode nanosecond laser pulse, one can easily calculate how the focal spot moves in time quantitatively.[21,30]

That the moving focus model can in fact explain the observed "filaments" with nanosecond laser pulses was first shown by Loy and Shen,[21,31,32] by Zverev et al,[33] and by Korobkin et al.[34] The latter used a streak camera to demonstrate explicitly the backward motion of the focal spot. Loy and Shen[31,32] showed that under appropriate conditions the focal spot can also move in the forward direction. Their experimental results agree quantitatively with the theoretical prediction. They also showed that the forward-moving focal spot can lead to partial trapping or nonlinear diffraction of light in the dielectric channel induced by the focal spot, and is responsible for the observed spectral broadening in the "filament".[31,35] Other characteristics of the "filament" can also be understood with the moving focus model.[36] Thus, for the nanosecond case, the moving focus picture was finally established beyond doubt.

Meanwhile, for the observed laser-induced damage streaks in solids, there was always the question how a self-trapped filament could induce a streak of damage spots and still have enough energy to sustain self-trapping, but then it became clear that the moving focus could easily explain such a damage streak.[33,37,38] Using a streak camera, Zverev et al.[33] and Giuliano and Marburger[38] proved that the damage streak was indeed induced by a moving focus.

There have also been a series of self-focusing experiments using picosecond mode-locked pulses.[39-47] In both solids,[39,42,44] and Kerr[39-41,45,46] and non-Kerr liquids,[39,43,47] "filaments" have been observed. Their general characteristics are qualitatively similar to those observed in the nanosecond case. However, because of the ultrashort laser pulsewidth, the self-focusing process is expected to be somewhat different. In Kerr liquids, self-focusing should now be governed by the transient response of the medium; self-focusing of the lagging part of the pulse is affected by the refractive index induced by the leading part of the pulse.[31,35,48,49] Akhmanov et al.[48] showed by approximate analytical solution and Shimizu[50] by numerical solution that in this case, after a certain distance in the medium, the deformed laser pulse tends to stabilize itself and can then propagate over a long distance without appreciable change in its spatial profile. This is called dynamic trapping, in contrast to self-trapping, proposed earlier.[1,7] Fleck and Carman[51] also did the numerical calculations for this case.

Quantitative measurements on transient self-focusing in Kerr liquids have been impeded by the slow advance in picosecond technology. More recently, Wong and Shen[52] have found a large field-induced refractive index and a long relaxation time (40 nsec - 1 μsec) in an isotropic liquid crystalline substance. It then becomes possible to study transient self-focusing quantitatively with Q-switched pulses and ordinary electronic detection system. Their results[53] agree very well with the dynamic trapping model, although in this case the spectral broadening is not appreciable since the phase modulation is slow.

Both the moving focus model in the quasi-steady-state case and the dynamic trapping model in the transient case fail to explain the observed filament diameters. The reason is clear. In the simple models, it is assumed that no other nonlinear process is present as the beam self-focuses. However, in reality, the high laser intensity in the focal region can initiate many nonlinear optical processes which in turn may prevent the beam from further self-focusing and limit the diameter of the "filaments". Various authors have suggested different mechanisms for limiting the filament diameter, such as multi-photon absorption,[26,54] forward[55] and backward[56] stimulated Raman scattering, optical breakdown,[57] etc.[58] It is possible that different mechanisms are actually responsible for the limiting diameter in different cases. Further investigation is necessary to resolve this mystery.

The self-focusing of light in gases has also been observed with nanosecond pulses.[59] Here, the nonlinearity arises from saturable absorption,[60] and the response of the medium to the field is nearly instantaneous. In addition, no other nonlinear optical process is present to complicate the problem. This is an ideal case since the problem can then be solved exactly by numerical computation. Such a calculation is being carried out by Loy and Grischkowsky.[61] A more thorough experimental investigation on the problem is however yet to be performed.

II Basic Physical Description of Self-Focusing

In this section, we shall limit our discussion to the case where the response of the medium to the applied field can be considered as instantaneous. This is the quasi-steady-state limit of self-focusing.

(A) Physical Description. in the quasi-steady-state limit.

Consider a single-mode laser beam with a Gaussian transverse profile propagating into a medium whose refractive index is given by $n = n_0 + \Delta n\,(|E|^2)$, where Δn is the field-induced part. A number of different physical mechanisms can give rise to Δn ——— libration, reorientation and redistribution of molecules, electrostriction, deformation of electronic clouds, heating, etc. (see Refs. 3, 4, 25). For positive Δn, the central part of the laser beam sees a larger refractive index than the edge, and should propagate with a lower velocity than the edge. Consequently, as the beam traverses the medium, the original plane wave front gets more and more distorted, as shown in Fig. 3. Then, since the rays always propagate in a direction perpendicular to the wave front, the beam appears to focus by itself.

A beam with a finite cross-section will of course also diffract. Only when the self-focusing action is stronger than the diffracting action, can the beam self-focus. Otherwise, it will still diffract. In the presence of a positive Δn, the diffraction will of course be much weaker (we call it nonlinear diffraction.) We shall define the self-focusing condition more quantitatively later. Here, we only want to point out that the self-focusing action is proportional to $\Delta n(|E|^2)$ which normally increases with the intensity $|E|^2$, and the diffracting action is inversely proportional to the square of the beam radius. Therefore, as the beam self-focuses and shrinks, both the self-focusing action and the diffracting action should become stronger; but if the latter grows faster than the former, then sooner or later, diffraction will overcome self-focusing and the self-focused

beam will diffract. However, if the self-focusing action is always stronger than the diffracting action, then the beam should keep on self-focusing to a smaller diameter until some other nonlinear process sets in to terminate self-focusing. This happens when the field-induced refractive index is given by $\Delta n = n_2|E|^2$, where n_2 is a constant coefficient. (In fact, for most materials which have been studied, the higher-order $|E|^2$ terms are always negligible except perhaps in the focal region.) In that case, the cumulative action of the nonlinear effect makes the beam self-focus quite sharply and suddenly (See Fig. 1). Consequently, the focal position is fairly well defined. What happens to the laser light in the focal region and thereafter is at present still a subject for debate.

(B) Simple Formalism.

Formally, self-focusing is described by the nonlinear wave equation[1]

$$\nabla^2 E - (\partial^2/c^2\partial t^2)[(n_o + \Delta n)^2 E] = 0 \qquad (1)$$

assuming the field is always transverse. For quasi-monochromatic light propagating in the forward direction, the above equation can be approximated by a partial differential equation which is first order in z and t . In addition, if we neglect the higher-order terms in the differentiation, then in the reduced time coordinate $\xi \equiv t - zn_o/c$, we have steady-state wave propagation even though the input laser intensity may be varying with time, i.e., the wave equation becomes independent of time. Thus, inserting $E = A(\gamma,z,\xi)\exp[ikz - i\omega t + iks(\gamma,z,\xi)]$ in Eq. (1) and neglecting the higher-order terms, we can convert Eq. (1) into two coupled equations for A and s.[62]

$$\frac{\partial A}{\partial z} + \left(\frac{\partial s}{\partial r}\right)\left(\frac{\partial A}{\partial r}\right) + \frac{A}{2}\left(\frac{\partial^2 s}{\partial r^2} + \frac{1}{r}\frac{\partial s}{\partial r}\right) = 0 \tag{2a}$$

$$2\left(\frac{\partial s}{\partial z}\right) + \left(\frac{\partial s}{\partial r}\right)^2 = 2\frac{\Delta n}{n_o} + \frac{1}{k^2 A}\left(\frac{\partial^2 A}{\partial r^2} + \frac{1}{r}\frac{\partial A}{\partial r}\right) \tag{2b}$$

(C) Self-Focusing Versus Self-Trapping.

The phase function $s(r,z)$ actually describes the wavefront of the beam. Equation (2b) shows how self-focusing and diffraction (the first and second terms respectively on the right-hand side of the equation) distort the wavefront. It is then clear that if we have at $z = z_o$,

$$2\frac{\Delta n}{n_o} + \frac{1}{k^2 A}\left(\frac{\partial^2 A}{\partial r^2} + \frac{1}{r}\frac{\partial A}{\partial r}\right) = 0 \tag{3}$$

for all r, then s at $z = z_o + \Delta$ only depends on $s(r,z)$ at $z = z_o$. For example, if at z_o, $\partial s/\partial r = 0$ for all r, then from Eqs (2a) and (2b), we find $\partial s/\partial z = 0$ and $\frac{\partial A}{\partial z} =$ for $z > z_o$. This corresponds to self-trapping; the wave propagates with both its amplitude and its phase (s) unchanged. However, to satisfy Eq. (3) for all r, even with $\Delta n = n_2|E|^2$, the amplitude function A must have a special form, as shown by Chiao et al.[1] For any other form of A, one may find that the left-hand quantity in Eq. (3) is positive for one region of r and negative for other region. As a result, one part of the beam self-focuses and the other part diffracts. This happens, for example, to a beam with a Gaussian profile.[26,27] Above a certain power threshold, although the central part of the Gaussian beam self-focuses, the

edge of the beam is still diffracting.

The satisfaction of Eq. (3) is often used as the condition for the initiation of self-trapping.[1] However, we want to emphasize here that the mere satisfaction of Eq. (3) at $z = z_o$ does not guarantee the initiation of self-trapping. We must have in addition $\partial s/\partial r = 0$ for all r at $z = z_o$. That the condition for steady-state self-trapping is so stringent makes self-trapping difficult to realize in practice. In fact, one can show that the self-trapping solution of Eq. (1) is an unstable one,[36,63] at least for the case of $\Delta n = n_2 |E|^2$ where a self-trapping solution has been found.

(D) Solution of the Wave Equation.

The analytic solution of Eqs. (2) is difficult to obtain. For the simple case of $\Delta n = n_2 |E|^2$, paraxial approximation has been used to solve the equations analytically,[48, 63,64] but the solution is only approximately valid in the region close to the beam axis. The equation can however be solved numerically on computers, at least in the prefocal region. (There is some difficulty in carrying the calculation through the focal region when the focal spot appears to be a singular point.) This has been done by several authors.[13,26,27,65] Goldberg et al.[26] and Dawes and Marburger[27] have found the numerical solutions for an input laser beam with a Gaussian profile over a wide range of input power P. In the case of $\Delta n = n_2 |E|^2$, they show that for $P > P_z \approx P_{cr}$, the beam will self-focus in such a way that the on-axis intensity increases sharply to infinity as z approaches the self-focusing distance z_f. The critical power P_{cr} is the same as the critical power for self-trapping defined by Chiao et al.

$$P_{cr} = (1.22\lambda)^2 \, c/128n_2 \tag{4}$$

where λ is the wavelength in vacuum. In Fig. 4, z_f as a function of P is shown.[27] For $P \gtrsim 1.2\, P_{cr}$, the curve can be well approximated (within 10%) by an asymptotic line given by the equation

$$z_f(t) = K/[\sqrt{P(\xi)} - \sqrt{P_o}\,] \tag{5}$$

where $\xi = t - z\, n_o/c$, $P_o = (0.858)^2 P_{cr}$, $K = 0.369\, ka^2\sqrt{P_{cr}}$ and a is the variance of the Gaussian profile. The on-axis intensity as a function of z can be approximated by

$$I(z,t)/I(0,\xi) = [1 - (z/z_f)^2]^{-\alpha/2} \tag{6}$$

where α is a parameter which depends on P as shown in Fig. 5.

Using a different numerical computing scheme, Dyshko et al.[29] have found that for $P \geqslant 2P_{cr}$, different annular parts of the beam would focus at different points as a result of nonlinear aberration, giving rise to multiple focal spots on the axis, but the position of the first focal spot is still given by Eq. (5). For $P_{cr} \leqslant P \leqslant 2P_{cr}$, only one focal spot exists.

Presumably, Eq. (5) is also valid for a beam profile which does not deviate too much from a Gaussian distribution. The coefficients K and P_o will of course be somewhat different for different beam profiles. They actually characterize the self-focusing process of a given single-mode laser beam in the nonlinear medium, and can be obtained directly from measurements[14] as we shall see later.

We next consider what happens to the self-focused light in

the focal region. The approximation of $n = n_2|E|^2$ is valid when $|E|^2$ is not too strong, but upon self-focusing, the continuous sharp increase of the field intensity as $z \to z_f$ will sooner or later cause Δn to saturate and diffraction to overcome self-focusing. The self-focused beam would finally diffract after it shrinks to a certain minimum diameter.[26,27] This is known to have happened to self-focusing in alkali vapor.[59] However, in liquids and solids, apparently before Δn gets saturated, other nonlinear optical processes would set in to terminate the self-focusing process and limit the minimum beam diameter. We shall come back to this problem in a later section for a more detailed discussion. In any case, experimental results seem to suggest that the beam diffracts soon after it reaches the minimum diameter, although the diffraction may be nonlinear[32] (see more discussion later). The focal region has a very small dimension (< 1 mm longitudinally) and can be appropriately called a focal spot at z_f.

(E) Moving Foci

We see from Eq. (5) that z_f is a function of time if the input power P varies with time. For a given input laser pulse, we can readily find $z_f(t)$ if K and P_o are known. An example is given in Fig.6., where we have also shown how the curve is constructed in a way which is physically transparent.[35] At t_A, the beam entering the medium at z = o has a power P_A; it travels with light velocity in the medium (along the dashed line in Fig.6) and finally self-focuses at $(z_f)_A$ (point A in Fig.6). At a later time t_B, the beam with a power P_B again propagates with light velocity in the medium and self-focuses at $(z_f)_B$

(point B in Fig.6), but since P_B P_A, we should expect $(z_f)_B<(z_f)_A$. Similarly, we can find the other focal points corresponding to different input powers at different times. The U curve is then obtained by connecting the various focal points in Fig.6. It is obvious from such a construction that the general shape of the curve should remain the same for a bell-shaped input pulse even if Eq.(5) does not hold.

The U curve in Fig.6 actually describes the motion of the focal spot. In a sufficiently long medium, $\ell > z_D$, the focal spot first appears at z_D. It then splits into two: one first moves backward, and then forward after it reaches a minimum self-focusing distance corresponding to the peak power of the pulse; the other keeps on moving forward with a velocity faster than light. Of course, the fact that the focal spot can have a velocity faster than light does not violate the special theory of relativity since nothing real is propagating along with the focal spot. However, a large polarization is actually induced in the focal spot. It now also has an apparent velocity larger than light velocity. This is then similar to the case of Cerenkov radiation. Therefore, in the present case, we should also expect to see a cone of radiation at an off-axis angle.[66] Whether this explains the occasionally observed anomalous rings around the "filament" is still to be investigated.

As suggested by Lugovoi et al.,[29] the moving focal spot is responsible for the observed "small-scale filament". Since the velocity of the focal spot is of the order of the light velocity, if a side-view picture of the focal-spot motion is taken

with an ordinary camera, what one obtains is just a bright filament with a diameter given by the diameter of the focal spot. However, a fast streak camera should be able to resolve the focal-spot motion.[34] In fact, with the help of the U curve, we can explain all the clean observations about the "small-scale filaments" in ordinary Kerr liquids under nanosecond pulse excitation.[36] These include the qualitative features of stimulated scattering and spectral broadening of light in the "filaments." We shall postpone the detailed discussion to the next section.

In all the above discussion, we have assumed instantaneous response of Δn to the field. This is clearly a good assumption in the prefocal region for an incoming pulse much longer than the relaxation time of Δn. In the focal region, however, because of the rapid motion of the focal spot (see Fig.6), the field intensity at a local point may vary appreciably during the relaxation time of Δn. Consequently, the transient response of Δn becomes important and affects the diffraction of light from the focal region.[32,35] This together with the occurrence of other nonlinear optical processes in the focal region makes the understanding of dynamics of self-focusing and nonlinear diffraction in and beyond the focal region extremely difficult.

If the input pulse has a width comparable to the relaxation time, then the entire self-focusing process is governed by the transient response of Δn. In order to find the transient self-focusing dynamics, Eq. (1) should now be solved in couple with the equation of motion for $\Delta n\ (\vec{r}, t)$. This has been done by several authors.[48-51,67]

We shall postpone the discussion to Sec. V and VI.

In the following section, we shall describe the various experimental observations and theoretical interpretations on quasi-steady-state self-focusing in an ordinary Kerr liquid.

IV Quasi-Steady-State Self-Focusing in Kerr Liquids with Nanosecond Laser Pulses.

In the earlier experiments on self-focusing, Q-switched laser pulses were used. The pulsewidth was much longer than the relaxation time of the Kerr effect of ordinary liquids which have been studied. Consequently, our previous discussion on quasi-steady-state self-focusing would apply. However, as we shall see more quantitatively later in this section, the dynamics of self-focusing and some characteristics of the "filaments" depend critically on the characteristics of the input laser pulse. Unfortunately, in all the earlier experiments, the characteristics of the input laser pulses were never carefully measured. The interpretation of those results then becomes impossible. Different research groups obtained different results on the filament characteristics without knowing that the differences came from the difference in input laser pulses. This created a great deal of controversy and bestowed on the field an ill reputation. In fact, most of these earlier experiments were done with multimode laser pulses which upon self-focusing gave rise to a large number of filaments. It was then impossible

to find the input condition for the formation of any individual filament.

In this section, therefore, we will only try to explain these earlier results qualitatively when possible. We shall discuss in more details the results obtained with single-mode laser pulses of known characteristics. Here, we should again emphasize that what we meant by a single-mode laser pulse is a TEM_{oo} pulse which will self-focus into only one single "filament", at least when the peak power is not very much higher than the critical power P_{cr}. Normally, a TEM_{oo} pulse with some weak ripples (which are difficult to detect) on it can be accepted as a single-mode pulse for other nonlinear optical experiments such as harmonic generation. In self-focusing, however, the weak ripples are readily amplified into multiple "filaments". Bispalov and Talanov[68] have shown that a beam with an intensity F in a nonlinear medium with $n = n_o + n_2|E|^2$ is unstable against spatial intensity variation with a characteristic size

$$\Lambda = \lambda_o c^{1/2}/(16\pi n_o^2 n_2 F)^{1/2}. \qquad (7)$$

If $F = 50$ MW/cm^2 and $n_2 \approx 10^{-11}$esu (for CS_2), we have $\Lambda \approx 100$ μm. This means that a small ripple of this size may cause the local part of the beam around the ripple to self-focus independently from the rest of the beam. Chiao et al. discussed the same effect from stimulated light scattering point of view.[69] This instability was demonstrated by Carman et al.[70] and more recently by Campillo et al.[71] The local bumps in the spatial intensity distribution may also show up as narrow spikes in time even though the power variation of the whole beam appears to be fairly smooth. Abbi and Mahr[72] have obtained direct experimental evidence of the correlation between filaments and intensity spikes.

We shall now begin describing the various experimental work on self-focusing in this quasi-steady-state limit and show how we can understand most of the results quantitatively.

(A) Self-Focusing in the Prefocal Region.

The first experiment on self-focusing dynamics was performed by Garmire et al.[15] In order to look at the beam profile at various points along the axis in the liquid cell, they used a number of mylar films immersed in the cell as beam splitters to couple some light out to be photographed. They found that at a certain distance, which is close to the predicted self-focusing distance, the beam diameter suddenly shrank to about 50 μm. However, limited by the technique and by the multimode laser they used, they did not study the detailed self-focusing dynamics in the prefocal region. In fact, it was found later that this 50 - μm "large - scale filament" they observed was actually composed of many "small-scale filaments" of few μm in diameter.[16]

The first quantitative study on the self-focusing dynamics in the prefocal region was done by McAllister et al.[23] with a single-mode ruby laser. They measured the on-axis intensity at the end of the liquid cell as a function of input power, and found that the results agree well with the theoretical calculation using Eq.(1) or (2) with $\Delta n = n_2|E|^2$ for quasi-steady-state self-focusing. (See Fig.7) In particular, they showed that by collecting only light which passes through an on-axis pinhole at the end of the cell, pulse sharpening occurred as the beam self-focused.[28] Later, Maier et al.[24] made a similar investigation with a single-mode laser

and extended the measurements up to the power at which the "small-scale" filament finally appeared. They found again good agreement between theory and experiment for self-focusing in the prefocal region. It is then clear that for nanosecond pulse excitation in ordinary Kerr liquids, the quasi-steady-state theory with $\Delta n = n_2|E|^2$ describes correctly the self-focusing dynamics in the prefocal region.

Most of the self-focusing experiments used linearly polarized laser light, and the light coming out from the region was also linearly polarized. However, Close et al.[73] showed that even if circularly polarized laser light was used, the light from the focal region (or the "filament") was still linearly polarized. This can be understood as the result of nonlinear coupling between the two circular polarizations through the field-induced refractive indices.[73]

$$\Delta n_{\pm} = (2\pi/n)[AE_{\pm}E_{\pm}^{*} + (A+B)E_{\mp}E_{\mp}^{*}] \qquad (8)$$

where the subindices "+" and "-" refer to the two circular polarizations and A and B are the two coefficients. For ordinary liquids, $A < A + B$, and hence the weaker one of the two circular components will self-focus first and become stronger. Since in practice, the input beam can never have perfect circular polarization, the weak component will always grow in intensity in the self-focusing process until the two circular components have equal amplitude.[73] The quantitative solution of this problem has not yet been worked out.

B General Characteristics of "Small-Scale Filaments"

Chiao et al.[16] first found the existence of "small-scale

filaments" in a self-focused beam. They observed that in a given Kerr liquid, the "filaments" have nearly the same diameter and the same intensity, independent of the input conditions as long as the input power is above the self-focusing threshold. Side-view photographs by Brewer et al.[17,19] showed that these filaments of constant diameter last over a distance of a few cm. These observations, made with multimode Q-switched ruby lasers, were then believed to be a manifestation of the self-trapping phenomenon predicted earlier.[1, 3,7] Later, they were shown to be due to moving foci.

The filaments and their formation have the following general characteristics in a Kerr liquid.[19,36]

1) Self-focusing of a multimode laser beam gives rise to multiple filaments, but, at least for $P < 10\,P_{cr}$, self-focusing of a single-mode laser beam leads to only one single filament. (Fig. 2 shows the end-view picture of a typical filament.)

2) When the cell length ℓ is very close to $z_f(P_{max})$, the diameter of the single-mode beam profile depends critically on the input power, but as ℓ or P_{max} increases, it soon decreases to a limiting size. (Fig. 2)

3) The limiting diameter is of a few μm, and is constant to within ± 20%.

4) If ℓ is larger than ~ 100 cm., the filament is likely to disappear at the end of the cell.

5) The filament is linearly polarized, independent of the polarization of the input beam for the reason mentioned earlier in Sec. IVA.

6) Δn in the filament is of the order of 10^{-3}, close to the value predicted by $n = n_2|E|^2$.[19,74]

7) If a photodetector is used to collect only light diffracted from the filament within a few cm near the end of the cell, then the observed light pulse has a pulsewidth which varies from ~ 200 ps when $z_f(P_{max}) \approx \ell$ to less than 100 ps when $z_f(P_{max})$ is appreciably smaller than ℓ. The energy density in such a pulse is few J/cm^2 (~ 4 J/cm^2 for CS_2 and toluene).

8) When $z_f(P_{max})$ is appreciably smaller than ℓ, the intensity of the filament is approximately constant (tens of GW/cm^2) for a range of P_{max}.

9) The filament diameter in liquid mixtures varies smoothly from one limiting value to the other as the composition of the mixtures changes from one limit to the other.

10) The spectral broadening of light from a filament depends critically on the characteristics of the input pulse, and is more appreciable for liquids with larger n_2.

Limited by available instruments, most measurements of the filament characteristics have not been very accurate. Better results can be expected with the help of the new fast streak cameras[75] and more sensitive photodetectors.

C. Evidences of Moving Foci Constituting the "Filaments".

As discussed in Sec. III, it seems more reasonable to interpret the observed "small-scale filaments" as the tracks of moving foci, although before 1969, the filaments were believed to be due to self-trapping. In this section, we shall review the experimental evidences for the moving-focus picture.

The first evidence is an indirect one found by Loy and Shen.[21] They took an end-view picture of the filament, but instead of focusing the camera at the end of the cell, they focused it into the cell, at few mm away from the end. If a moving focus is responsible for the filament, this change of focusing should not distort the image. However, if the filament is a self-trapped filament, then the image should be distorted because of refraction and reflection of light in the filament. The experiment showed that the former is true. They also found that only when $\ell \rightarrow z_f(P_{max})$ a bubble was generated in the liquid by the laser pulse at the end of the cell. This can be considered as another evidence for the moving focus. As seen in Fig.6, the moving focus spends a much longer time around $z_f(P_{max})$, and can therefore deposit enough energy through optical breakdown or ionization in that local region to create the bubble.

The direct evidence of a moving focus was first obtained by Korobkin et al.[34] using a streak camera. Their motion picture showed a clear backward moving focus. One would expect the backward moving focus to turn around at $z_f(P_{max})$ and move forward. The fact that this has not been observed can be understood as follows.[32] Stimulated Raman and Brillouin scattering is initiated at the focus all along the filament. As shown in Fig.8, the backward Raman and Brillouin radiation should propagate along the dashed-dot lines with its wavefront initiated at E. It intersects the incoming laser light before the latter self-focuses and through

amplification, effectively depletes the laser power.[76] Consequently, the incoming laser beam may no longer have enough power to self-focus, and the motion of the focus is terminated.

Figure 6 shows that one should also see a forward moving focus if the cell is long enough. For a reasonable cell length ($\ell < 100$ cm) and a laser pulse with low peak power ($P_{max} \approx 2P_{cr}$), this can be achieved if K in Eq. (5) is relatively small. Assuming a 10 ns input pulse with a transverse Gaussian profile, we find $K/\sqrt{P_{cr}}$ should be around 4 cm (corresponding to $z_f(P_{max}) \approx$ 10 cm) or the beam radius a (variance of the Gaussian profile) should be about 100 μm. The experiment was carried out by Loy and Shen[31] using a single-mode Q-switched ruby pulse with a peak power of about 100 kW and a radius of about 150 μm propagating in a 36 cm toluene cell. They first measured the threshold power for self-focusing at various cell lengths, i.e., $\ell = z_f(P_{max})$ as a function of P_{max}. The data plotted as $1/z_f(P_{max})$ versus $P_{max}^{1/2}$ appeared to be a straight line from which they could deduce K and P_o using Eq. (5), as was done by Wang.[14] (Fig. 9) Then, knowing P(t) from the oscilloscope trace for a given input pulse, they were able to plot the entire U curve using Eq. (5). A section of it is shown in Fig. 10 for a typical input pulse (~ 8 ns in pulsewidth). It is seen that if the cell length is larger than 23 cm, then one should find a focal spot which starts at 23 cm and moves forward towards the end of the cell with a velocity faster than the light velocity. In order to prove this experimentally, they inserted a 100 μm microslide at a certain distance in the cell. When the focal spot hit the microslide, it created a short pulse of diffracted

light. They could then measure the time delay between this pulse and the pulse created when the focal spot hit the end window. It was found that the time delay was positive indicating a forward moving focal spot. In addition, the delay was smaller than the distance between the microslide and the end window divided by the light velocity, showing that the focal spot was indeed moving faster than light. The measured time delay also compared well with the value predicted by the U curve as shown in Fig. 10. This quantitative agreement between theory and experiment therefore proves conclusively the moving focus model.

One may raise the question whether the microslide would diffract the self-focused light and affect the results in the above time-of-flight measurement, but it is clear that because of the sharp focusing, a 100 μm microslide cannot appreciably change the position of the focal spot at 10 cm away from the microslide. However, Loy and Shen[32] performed another time-of-flight measurement on the moving focus without any microslide in the cell. They measured the time delay between the backward Raman pulse and the short pulse of diffracted light created when the focal spot hit the end window. From the delay, they could locate where the Raman pulse was initiated. On the other hand, it is known that the short backward Raman pulse is created by continuous amplification of the wavefront of the backward Raman radiation.[76] Therefore, knowing the U curve, they could also predict where the backward Raman pulse was initiated. Comparing the two results, they found good agreement as shown in Fig. 11 for various input powers and cell lengths. This gives

further strong support of the moving focus model.

The moving focus model can also explain qualitatively or semi-quantitatively the other observation on "filaments" generated by nanosecond input pulses. For example, from the U curve, we can see that if the photodetector collects only light diffracted from the focal region in the last few cm of the cell, then the observed light pulse can only be about 100 ps long; the pulse should be longer if $\ell \approx z_f(P_{max})$. These predictions agree well with observations.[21,36] If z_f is large, the focus would become long (approaching infinity as $z_f \to \infty$). Then, the laser light is likely to be all converted into Raman and Brillouin radiation in the focus. This explains the disappearance of the filament at the end window if ℓ is too large. We shall discuss how the moving focus model explains the other experimental observation on filaments in the following sections.

D. Relation between Self-Focusing and Stimulated Raman and Brillouin Scattering.

The sharp stimulated Raman threshold and the anomalously high Raman gain in Kerr liquids were a big mystery around 1965. We now understand that they are due to self-focusing. Because of the high laser intensity, both stimulated Raman and stimulated Brillouin scattering are readily initiated in the focal region. The sharp Raman and Brillouin thresholds should therefore nearly coincide with the self-focusing threshold.

Experiments have been performed trying to correlate more

precisely self-focusing with stimulated Raman and Brillouin scattering.[24,36] In CS_2 and toluene, it was found that stimulated Raman and Brillouin scattering do not have the same threshold. The Brillouin radiation first shows up above the detectable level when the self-focused beam has shrunk to a diameter of about 50 μm. Then, the Raman radiation appears after the beam has self-focused to within a factor of 2 of the limiting diameter. This can be understood by the fact that stimulated Brillouin scattering has a slow transient response (~10 ns for acoustic response time) while stimulated Raman scattering has a nearly instantaneous response (~ 5 ps for vibrational lifetime), but the latter has a much smaller steady-state gain.[24] As the laser intensity increases upon self-focusing, the Brillouin radiation has initially a higher gain and therefore reaches the detectable level first before the Raman does. Subsequently, further focusing of the beam increases the light intensity very quickly and also increases the Raman gain proportionally. The Brillouin gain, however, cannot follow the rapid change of the field intensity and now falls below the Raman gain. In that region, the Raman effect appears to be dominant.

The above argument can also be used to understand a number of other experimental observations. Figure 12 (for the case $\ell < z_D$ in Fig.6, so that the upper branch of the U curve is absent) shows that the incoming laser pulse is effectively depleted by the backward stimulated Raman and Brillouin scattering.[76] When the laser power first reaches the self-focusing threshold, the transient

stimulated Brillouin scattering does not deplete the laser power appreciably. Therefore, the incoming laser beam continues to self-focus to a smaller diameter. Then, once the stimulated Raman scattering is initiated, the large gain in the focal region and the quick Raman build-up soon deplete the incoming laser power effectively below the self-focusing threshold, creating the sharp dip in the transmitted laser pulse in Fig.12. Termination of self-focusing also stops the backward stimulated Raman scattering, and the incoming laser power recovers its strength. When the laser power again reaches the self-focusing threshold, Brillouin radiation is again initiated first, but now, it also has a large enough transient gain to deplete the incoming laser power effectively. Thereafter, by self adjustment, the backward stimulated Brillouin scattering keeps the transmitted laser power always close to but below the self-focusing threshold. If the transmitted laser power is too high, the stimulated Brillouin scattering would increase to deplete more laser power. If the transmitted laser power is too low, the stimulated Brillouin scattering would decrease to let more laser power get through. Thus, the transmitted laser power is no longer strong enough to self-focus to the limiting focal diameter and hence stimulated Raman radiation can no longer be initiated. The moving focus (or filament) is also effectively terminated as mentioned earlier in Sec. IV C. This explains the flat top of the transmitted laser pulse and the fact that after the short Raman pulse, the sum of the transmitted laser power and the backward Brillouin power is equal to the incoming laser power, as shown in Fig.12.

The extremely short backward Raman pulse is also understood as due to the fact that the wavefront of the backward Raman radiation continuously meets the fresh incoming laser light and gets amplified through depletion of the laser power.[76] We now know that this Raman wavefront is initiated either at the end of the cell when $\ell < z_E$ or at z_E if $\ell > z_E$ (see Fig. 8).[32] Therefore, in order to have a shorter Raman pulse and a higher peak power, we should have a longer interaction length for the backward Raman amplification; in other words, either ℓ or z_E, whichever is smaller, should be larger while the input laser intensity remains unchanged. As seen from Eq. (5), this can be achieved with a larger input beam radius. On the other hand, if the cell length is fixed, then the increase of input laser power would not increase the interaction length appreciably, and the backward Raman pulse would remain nearly unchanged. This is in fact what was observed when the laser power was increased above the self-focusing threshold.[36]

The forward Raman radiation is initiated and amplified in the focal region and gets further amplified while propagating along with the diffracted laser light. Because of the shorter interaction length, the forward Raman pulse is much weaker than the backward Raman pulse just above the threshold. As the input laser power or the cell length increases, the forward Raman light increases steadily because of a longer interaction length and because of a longer section along the axis where stimulated Raman scattering is initiated. Since the backward Raman pulse soon becomes saturated for the reason mentioned earlier, the forward Raman

pulse may eventually have more energy than the backward one, although it may not be as short as the latter.[77] This explains qualitatively the anomalous forward-backward ratio of the stimulated Raman radiation observed before self-focusing was recognized.[8,76] An example is shown in Fig. 13.[77] Since the forward Raman radiation is generated mainly from the focal region, if we collect only light diffracted near the end of the cell (say, within 2 cm.), we should expect to find a forward Raman pulse as short as the diffracted laser pulse and also coincident in time with the latter. This was actually observed in the correlation measurements.[36] The forward Raman scattering can also deplete the laser power in the focal region effectively. It was found that in some cases, practically only forward Raman light but no laser light was diffracted from the filament inside the cell.[36]

There are a few other observations on Raman and Brillouin pulses. All of them can be explained qualitatively by the moving focus model.[36] In principle, one can find quantitatively the solution of stimulated Raman and Brillouin scattering by solving the nonlinearly coupled wave equations for the laser, the Raman, and the Brillouin fields. However, this is a difficult job even with the largest and fastest computer available. Hopefully, the qualitative understanding of Raman and Brillouin generation we have outlined here can help in making appropriate physical approximations to simplify the solution of the equation.

E. Spectral Broadening of Light from a "Filament"

If the spectrum of light emitted from a filament is analyzed

one often finds appreciable spectrum broadening relative to the spectrum of the incoming laser light.[78-82] Even with single-mode laser excitation the spectral broadening can be as large as several hundred cm^{-1} and usually has a characteristic semi-periodical structure (Fig. 14a). This result was interpreted as due to self-phase-modulation of light in a self-trapped filament.[79,80,83] The basic idea was as follows:[79] Assume the laser pulse propagating in a self-trapped filament has a bell-shaped time-variation $|E^2(t)|$. The corresponding field-induced refractive index is $\Delta n(t) = n_2|E(t)|^2$ (assuming instantaneous response). Because of $\Delta n(t)$, the self-trapped light, after propagating through a filament of length L, acquires a time-dependent phase increment $\Delta\phi(t) = (\omega/c)L\,\Delta n(t)$. This phase modulation in turn gives rise to a frequency modulation $\Delta\omega(t) = -\frac{\partial}{\partial t}[(\frac{\omega}{c})\ell\,\Delta n(t)]$. The maximum of $\Delta\omega(t)$ appears when the slope of $\Delta n(t)$ or $|E(t)|^2$ is a maximum, and represents the extent of spectral broadening. Furthermore, on a bell-shaped curve, there are two points of the same slope i.e., two fields at two different times with the same $\Delta\omega$. These two fields can interfere constructively or destructively, creating peaks or valleys respectively in the power spectrum. This then explains the semi-periodic structure of the spectral broadening. More generally, one can include the transient response of Δn to the pulse field in the calculation. The net effect of the transient response of Δn is to reduce the spectral broadening on the anti-Stokes side with respect to the Stokes side.

Using the pulsewidth W and the filament length L as adjustable parameters, (W ~ a few picoseconds and L ~ a few centimetres),

Gustafson et al.[83] showed that the calculated spectrum agreed very well with the observed one. (Fig.14b). Because of this apparently successful interpretation, spectral broadening had always been used as the major evidence to support the self-trapping model. It is however difficult to understand how the self-trapped filament is formed and why only a few ps portion of the few ns Q-switched pulse is being self-trapped in the filament.

As demonstrated by Shen and Loy,[35] we now know that a moving focus can also induce phase modulation and hence spectral broadening. With essentially no assumption, they can predict semi-quantitatively the spectral broadening from a given input condition. The predictions are in good agreement with experimental results. The basic theory is as follows.[35]

We must show that the light emitted from the axial region at the end of the cell is in fact phase modulated in time. Figure 15 shows again the trajectory of the moving focus corresponding to a nanosecond input pulse. The beam entering the cell at time t_A propagates along the dashed line, self-focuses sharply at A (defined as the position where the diameter of the self-focused beam is minimum), and leaves the cell at A'. Knowing the self-focusing geometry, we can find the intensity distribution $|E(z,t)|^2$, and in particular, $|E(\ell,t)|^2$. From $|E(z,t)|^2$, we can obtain $\Delta n(z,t)$ from the relaxation equation

$$\frac{\partial(\Delta n)}{\partial t} + \frac{\Delta n}{\tau} = \frac{n_2}{\tau} \; |E(z,t)|^2 \qquad (9)$$

where τ is the relaxation time of the order of a few ps. in ordinary liquids (2 ps

for CS_2). We realize that $\Delta n(z,t)$ is only appreciable in the focal region (denoted by the shaded region around the U curve in Fig. 15) where $|E(z,t)|^2$ is large. The self-focused beam traversing the cell should now acquire a phase increment $\Delta\phi$ due to the presence of Δn. From Eq. (2b), we find (at r=o)

$$\Delta\phi(t = t_A + \ell n/c) = \int_o^\ell \left(\frac{\omega}{c}\right) \Delta n_{eff}\,(z,t' = t_A + zn/c)dz \qquad (10)$$

where $\Delta n_{eff} \simeq \Delta n - 2n_o/k^2r_o^2(z,t)$ assuming that the transverse field profile can be approximated by a Gaussian with γ_o being the variance. This second term in Δn_{eff} is due to diffraction. Eq. (10) shows explicitly that the light emitted from the axial region at the end of the cell is phase modulated. From $|E(\ell,t)|^2$ and $\Delta\phi(t)$, we can then obtain the power spectrum by Fourier transform.

Let us now be somewhat more quantitative. We know that in the focal region, the pulsewidth of $|E(z,t)|^2$ is of the order of the relaxation time τ. It cannot be much smaller since the observed Δn_{max} is not much less than the steady-state value $\Delta n_o = n_2|E(z,t)|^2_{max}$. It cannot be much longer since otherwise the stationary self-focusing theory would hold even in the focal region and would then predict a sharp focusing and a pulsewidth smaller than τ, contrary to the assumption. Therefore, in Fig. 15, the shaded region has a width of the order of τ, and essentially only light emitted from the shaded part at $z = \ell$ contributes to the power spectrum. To calculate the phase increment acquired by this part of the light, we can approximate the last

portion of the U curve towards the end of the cell by a straight line, and then the phase increment is given approximately by

$$\Delta\phi \simeq \left(\frac{\omega}{c}\right)\left(\frac{n}{c} - \frac{1}{v}\right)^{-1} \int_{t_o}^{t} \Delta n_{eff}(\ell,t')dt' \tag{11}$$

where v is the velocity of the focal spot towards the end of the cell and t_o is the time when $\Delta n(\ell,t)$ becomes non-negligible. The corresponding frequency modulation is

$$\Delta\omega(t) = -\left(\frac{\omega}{c}\right)\left(\frac{n}{c} - \frac{1}{v}\right)^{-1} \Delta n_{eff}(\ell,t) \tag{12}$$

and the maximum Stokes broadening is given by

$$\Delta\omega_{max} = -\left(\frac{\omega}{c}\right)\left(\frac{n}{c} - \frac{1}{v}\right)^{-1} (\Delta n_{eff})_{max}. \tag{13}$$

As seen from Eq. (13), the maximum Stokes broadening depends on the detailed self-focusing dynamics only through $(\Delta n_{eff})_{max}$, which is actually not very sensitive to the variation in self-focusing dynamics. For a rough estimate of $\Delta\omega_{max}$, we can let $(\Delta n_{eff}(\ell))_{max} \simeq \frac{1}{2}\Delta n_o = \frac{1}{2} n_2 |E(\ell,t)|^2_{max}$ where $|E(\ell,t)|^2_{max}$ can be obtained from the approximate relation $nc|E(\ell,t)|^2_{max} d^2/8 = P(z_f=\ell)$ where d is the filament diameter and $P(z_f=\ell)$ is the beam power which self-focuses at ℓ. For CS_2 and toluene with $\ell \sim 10$ cm, we have $\frac{1}{2}\Delta n_o$ approximately equal to 1.5×10^{-3} and 4×10^{-4} respectively. Therefore, in order to obtain a maximum Stokes broadening of about 100 cm^{-1} in CS_2 or 30 cm^{-1} in toluene, we must have $(n/c - 1/v)^{-1} = 7\ c/n$ or $= 1.15\ c/n$, i.e., the focal-spot velocity towards the end of the cell must approach the light

velocity. From Eq. (5), we find

$$\left(\frac{n}{c} - \frac{1}{v}\right)^{-1} = \left(\frac{\ell^2}{K}\right)\left[\frac{1}{P^{1/2}} \frac{dP(t)}{dt}\right]_{P = P(z_f = \ell)}. \tag{14}$$

This shows that for $v = 1.15\ c/n$ at $\ell = 10$ cm, we need an input pulse with a pulsewidth around 0.7 ns. The shorter the input pulse, the closer v approaches c/n and the larger $\Delta\omega_{max}$ becomes. On the other hand, if an ordinary Q-switched pulse of 10 ns pulsewidth is used, our estimate gives a spectral broadening of less than 10 cm^{-1} in CS_2 and less than 3 cm^{-1} in toluene. This is indeed what one observed in experiments. As reported in the literature,[31,79] whenever a single-mode Q-switched laser is used in the self-focusing experiments, spectral broadening of light from the filament is always not appreciable. With much shorter pulses, however, spectral broadening can readily be seen. Using a weakly mode-locked pulse of ~ 1.2 ns long, Wong and Shen[84] were able to verify eq. (13) semi-quantitatively. (Fig. 16).

Physically, the moving focal spot induces locally in the medium a Δn which lasts at least for several relaxation times; or one can imagine that there is a channel of Δn of several $\tau(\partial z_f/\partial t)$ long trailing after the focal spot. If the focal-spot velocity is larger than c/n but approaches c/n, then the defocused light from the focal spot will see over a relatively long distance an appreciable Δn and will diffract nonlinearly from the channel of Δn. Only in this ideal limiting case, the defocused light is completely trapped in the dielectric channel of

Δn. The result of nonlinear diffraction or partial trapping is to lengthen the trailing edge of the filament pulse $|E(\ell,t)|^2$ emitted at the end of the cell. This will change the absolute value of $(\Delta n_{eff})_{max}$ and hence $\Delta\omega_{max}$, but in general not by a factor of 2 or 3. The detailed forms of $|E(\ell,t)|^2$ and $\Delta\phi(t)$ are responsible only for the details of the semi-periodical structure in the broadened power spectrum. To find $|E(\ell,t)|^2$ and $\Delta\phi(t)$ rigorously, however, we have to solve Eqs. (1) and (9) coupled with other equations which describe the other nonlinear processes induced in the focal region. This is unfortunately a rather formidable task.

In Fig. 17, we show a calculated power spectrum of the filament obtained from a 1.2 ns input pulse in a 22.5 cm CS_2 cell.[35] The pulseshape $|E(\ell,t)|^2$ here was arbitrarily assumed with the restriction that the pulsewidth is not more than several τ. The corresponding phase increment $\Delta\phi(t)$ is then calculated (the diffraction effect is not included in this calculation). Finally, the power spectrum is obtained by Fourier transform which reveals the characteristic semiperiodic spectral broadening. It has been shown that the detail of the semi-periodic broadening does depend rather sensitively on the pulse-shape of $|E(\ell,t)|^2$, but the maximum Stokes broadening does not as long as $\Delta\omega_{max}$ is much larger than the inverse pulsewidth.[35] In this respect, it is interesting to note that while Gustafson et al.[83] have to assume a self-trapped pulse of few ps long in order to explain the observed spectral broadening, the output filament

pulse $|E(\ell,t)|^2$ in our model appears naturally a few ps long, as restricted by the relaxation time τ.

We show in Fig. 18 a typical experimental spectrum of a filament obtained with a single-mode 1.2 - ns laser pulse.[84] There is a strong central peak in the spectrum. This indicates that part of the light emitted from the filament has little phase modulation. It presumably comes from the periphery of the beam which self-focuses and diffracts sharply. In a longer cell and with a shorter input pulse, both self-focusing and nonlinear diffraction should appear to be more gradual, and the relative intensity of the central peak should reduce. In the limit of total trapping, we would expect to see only the broadened semiperiodic structure with no central peak. A calculated power spectrum is also shown in Fig. 18 for comparison[84]. In the calculation, the filament pulse is assumed to be a coherent superposition of a phase-modulated part and a phase-unmodulated part.

Under nanosecond pulse excitation, the spectral broadening on the anti-Stokes side is always much less and weaker. As seen from Eq. (12), the anti-Stokes broadening comes from the period when $\Delta n_{eff}(\ell,t)$ is negative. This corresponds to the region where the intensity $|E(\ell,t)|^2$ is low because of diffraction and depletion by other nonlinear processes. The maximum value of the negative $n_{eff}(\ell,t)$ is also expected to be small. Consequently, the power spectrum on the anti-Stokes side should be weak and should not extend very far.

Finally, we should mention that there are many earlier reports in the literature on the observation of spectral broadening of light

from a filament with Q-switched pulses.[78-82] The results were always interpreted using the self-trapping model. In retrospect, we believe that multimode lasers were used in these experiments, and the observed spectral broadening must come from the subnanosecond spikes in the Q-switched pulses. Unfortunately, the input conditions for the formation of each individual filament in these experiments cannot be deduced, and therefore no quantitative analysis using the moving focus model can be done to interpret the results of these experiments.

We shall postpone our discussion on spectral broadening under picosecond pulse excitation to Sec.VI.

F) Limiting Filament Diameter.

As mentioned earlier, the observed filament in self-focusing has a limiting diameter. From the moving focus model, we now understand that this limiting diameter corresponds to the diameter of the focal spot. However, the fact that the diameter is roughly a constant in a given medium, independent of the input conditions, is not yet clearly understood and is still a subject of controversy. The main difficulty is that in order to predict the filament diameter correctly, one must know the complete self-focusing dynamics through the focal region with all the other non-linear processes properly taken into account. There does not exist any reasonable approximation which one can make to circumvent this difficulty.

Several different mechanisms of limiting the filament diameter have been suggested by various authors. All of them aim for a limitation in the increase of Δn so that diffraction can overcome

self-focusing at a reasonable field intensity and beam diameter. We discuss these proposed mechanisms separately in the following.

1) Saturation of Δn for a Kerr liquid may occur in high fields as the molecules approach perfect alignment.[26,27,85,86] However, it has been shown for non-interacting molecules that this would happen at much larger Δn and $|E|^2$ than the values observed in a filament.[26,27,85] Even if the molecular interaction is taken into account, it is believed that $|E|^2$ required for saturation of Δn would be much larger than the field intensity in a filament.[86]

2) Steric and compressibility effects may prevent perfect alignment of molecules and make Δn appear to saturate at a much lower value.[58] The model calculation on Δn in this case has not been verified by experiment.

3) Two-photon absorption may effectively reduce the increase of Δn with the field intensity.[26] This is probably not the dominating mechanism for limiting the filament diameter in many Kerr liquids in which two-photon absorption is weak. Also, two photon absorption is probably not nonlinear enough to be the limiting mechanism.

4) Multiphoton absorption[54] and pre-breakdown[57,87] ionization may effectively reduce the increase of Δn with $|E|^2$. This is perhaps the limiting mechanism for the picosecond case, but for nanosecond pulses in liquids the field intensity at which these mechanisms become important may be somewhat too large compared with the observed value. Also, in practice, stimulated scattering appears in the focal region before multiphoton ionization becomes operative.

5) Stimulated Raman and Brillouin scattering may be responsible

in terminating self-focusing.[55,56] As discussed earlier, the backward stimulated Raman and Brillouin scattering can deplete the energy in the incoming laser beam and terminates self-focusing. It effectively eliminates the lower branch of the U curve for the moving focus. Even for the upper branch, it may carry away an appreciable portion of the energy in the self-focused beam and reduce its self-focusing action.[46] Recently, however, Rahn and Maier[55] have shown that the forward stimulated Raman scattering is more important in limiting the filament diameter, since it strongly depletes the laser energy in the self-focusing process, and reduces Δn through the following mechanisms: a) excitation of molecular vibration and hence a reduction of electromagnetic energy in the self-focused beam, b) strong conversion of laser light into Stokes light in the centre of the beam, and c) the diffraction of Stokes light out of the self-focused beam. By solving the coupled time-independent wave equations for the laser and the forward Stokes waves on a computer to find the self-focusing geometry, they obtain a minimum diameter for the self-focused beam. The incident laser power was chosen to have the limiting diameter reached at the end of a given liquid cell (l=30 cm). Then, the calculated limiting diameters are in good agreement with the observed ones for both pure liquids and liquid mixtures. Therefore, this explanation of the limiting diameter seems to be very plausible. However, from what we discussed earlier about the moving focus picture for nanosecond pulse

excitation, it is clear that self-focusing in the focal region is governed by the transient response of the medium. It is rather doubtful that the steady-state theory of self-focusing can correctly describe the real self-focusing dynamics. Rahn and Maier[55] also did not mention how the calculated limiting diameter varies with the cell length, while in practice, the observed filament diameter is nearly independent of the cell length.

Clearly, the subject is still open. It is most likely that in different cases, different nonlinear optical processes are responsible for the limiting diameter, but a convincing answer would require a full solution of the self-focusing dynamics taking into account all the relevant nonlinear processes.

A few words should also be said about the measurement of a filament diameter. Normally, it is done by taking a time-integrated photograph of the beam profile at the end of the cell. (Fig. 2) The filament diameter is then obtained from the densitometer trace of the filament on the photograph. A small disk is often used to block the unfocused light from reaching the camera. However, even if the unfocused light is not blocked, the filament can still show up clearly on the photograph. This is because it usually contains an energy density of few J/cm^2 which is much higher compared with the energy density of few tenths of a J/cm^2 in an unfocused laser pulse. Even though the unfocused background is not important, we should still keep in mind that because the photograph is a time-integrated one, the observed filament diameter

may be somewhat larger than the actual limiting diameter.

G) Discussion.

We have seen that for nanosecond pulse excitation, the moving focus model does give a consistent description of the "small-scale filament" which agrees qualitatively and sometimes quantitatively with what have been observed. Certain characteristics of the filaments depend critically on the input conditions, and hence it becomes impossible to explain quantitatively the earlier experimental results obtained with unknown input conditions. Nevertheless, most of these results can still be explained qualitatively by the moving focus picture. For example, Denariez-Roberge and Taran[82] found with a multimode laser the following results. About 50 filaments were observed in CS_2 with a laser beam of 500 um in diameter. The filaments were still present if a screen with 30 um holes was inserted in the cell. The number of filaments reduced by a factor of 3 when a 1 mm glass slide was inserted in the cell at 1.3 cm away from the end window. The observed spectral broadening increases with the length of a filament. These results can be explained by the moving focus model. The filaments were probably created by self-focusing of local intensity humps of 30 um or less in diameter in the laser beam. These humps could go through the screen without being blocked, but would be smoothed out by diffraction in passing through the 1 mm glass slide. Also, according to the moving focus model (Sec. III), a longer filament is obtained with a higher input power or a longer cell length. In both cases, one should expect to see a broader spectrum.[84]

There are of course still a number of problems on quasi-steady-state self-focusing which are unsolved. The controversy on the filament diameter is yet to be clarified. The self-focusing dynamics in the focal region is yet to be understood; in particular, how the beam diffracts from the focal region is not known. How stimulated Raman and Brillouin scattering depletes the laser energy in the focal region is also an interesting problem to solve. The observation of Stokes and anti-Stokes rings around the filaments has not yet been explained by the moving focus model. Our present knowledge about the characteristics of a filament has been limited by the speed and sensitivity of the detection systems. The recent advance on fast streak cameras[75] can of course greatly improve those measurements. A fairly accurate determination of $\Delta n\ (\vec{r},t)$ throughout the beam path would of course be most interesting.

V Self-Focusing of Nanosecond Pulses in Transparent Solids.

Hercher[5] first reported the observation of damage tracks in solids induced by high-power laser beams. These damage tracks are usually few microns in diameter and several cm long. It was soon recognized by Chiao et al[1] that self-focusing is probably the cause of these damage tracks. They proposed the self-trapping model in order to explain the filamentary characteristic of the tracks. There is however an obvious difficulty in their interpretation: a self-trapped light pulse cannot have sufficient energy to create a damage track of several cm long unless energy is constantly fed into the optical waveguide from the side. On the other hand, the moving focus model has no such difficulty since the beam energy is

constantly being fed into the focal region. Zverev et al[33] and Giuliano and Marburger[38] have in fact shown that the moving focus model correctly describes the formation of damage tracks, although the model needs some modification as we shall see.

Let us first give a brief description of the characteristics of the damage tracks in solids, as reported by Steinberg.[88] A damage track usually occurs in the form of a cylindrical region of altered refractive index, a few microns in diameter, straight to within an rms deviation of one wavelength, and up to 9 cm long. It always starts with a damage star and may disappear towards the exit face of the sample, but the exit surface usually has a pit on the extended axis of the track. Track formation is characterized by a flash of scattered white light from the track, an increase in the exit divergence angle of the laser beam, and a short pulse of backward stimulated Brillouin radiation. It is also accompanied by a detectable cylindrical sound wave. The damage threshold depends on the incident beam radius and pulsewidth. It is as low as 10 kW for a ruby laser beam sharply focused (~5 cm. focal length) in dense flint glass, and more than 2 mW for an unfocused beam in fused silica. With a single-mode laser beam, only one damage track can be observed from each laser pulse.[38]

If a streak camera is used to study the track formation, one can actually observe the damage spot (marked by the emission of broad-band light) propagates in the solid.[33,38] Giuliano and Marburger[38] showed that in their experiment with a Q-switched laser pulse in sapphire, the damage spot first appeared when the input

laser intensity was at the pulse waist, then travelled back towards the laser as the input intensity increased, and finally reached the end of the track at the peak of the input laser pulse. (See Fig. 19). The damage spot stayed at the end of the track for a relatively long time and created a damage star.

These results have been explained qualitatively by the moving focus model.[33,37,38] There is however an important difference between the present case and the case described in the previous section for Kerr liquids. In most solids, molecular libration, reorientation, and redistribution are frozen out, and the electronic contribution to the nonlinear refractive index is often negligible. Electrostrictive effect appears to be responsible for self-focusing.[1,2,67,89] But then, electrostriction has a response time longer than the pulsewidth of the input Q-switched pulses, and therefore, the quasi-steady-state theory of self-focusing described in Sec. III is not even valid in the prefocusing region.

The transient solution of self-focusing must be obtained by solving the wave equation (1) together with the equation of motion for Δn. In the present case, Δn is proportional to the density variation $\Delta\rho$ induced by electrostriction. The equation of motion for $\Delta\rho$, and also for Δn is simply the driven acoustic wave equation. In the small-amplitude approximation, we have

$$(\nabla^2 - \frac{1}{v_a^2}\frac{\partial^2}{\partial t^2} + \frac{2\Gamma}{v_a^2}\frac{\partial}{\partial t})\Delta n = \frac{n_o\rho_o}{4\pi v_a^2}\left(\frac{\partial n}{\partial \rho}\right)\nabla^2|E|^2. \tag{15}$$

It is seen that because of sound-wave propagation, $\Delta n(\vec{r} \cdot t)$

depends not only on the history of local intensity variation but also on the history of intensity variation at other spatial points. This makes the analysis of electrostrictive self-focusing more difficult.

We can however expect that as a result of the transient response of Δn, self-focusing and defocusing of the beam should be much more gradual than in the case of quasi-steady-state self-focusing.[49] A focus with a longitudinal dimension of a few cm would not be impossible. Then, at any instant, if we plot the beam radius along the axis, we may find a section of a few cm of nearly constant beam radius. Note that it is now only a problem of semantics to call it either a long focus or a trapped filament (dynamic trapping - partial beam trapping or nonlinear diffraction due to Δn induced by the earlier part of the beam).[31,48-51] These are in fact the results obtained by Kerr[67] from computer calculation.

When the focus is long, the definition of a focal spot becomes ambiguous. One can of course define the focal spot as the position of the minimum radius in the focus, but in fact, for self-focusing in solids, the more relevant quantity is the damage spot which appears whenever the local field intensity of the self-focused beam reaches the critical value. The damage would then effectively stop further self-focusing of the rays. Thus, the damage spot is well defined.[67] It moves along the axis in the solid as the input laser power varies with time. The trajectory of the damage spot can be plotted out if the axial intensity variation with time due to self-focusing is known. Since the self-focusing threshold depends

on the incident beam radius and pulsewidth, the damage threshold also does. The numerical solution of the damage trajectory has been worked out by Kerr.[67]

In some solids, the electronic contribution to the nonlinear refractive index is not negligible. Thus, in semiconductors, Tzoar and Gersten[90] have shown that the non-parabolicity of the bands or the velocity-dependent effective masses can give rise to a large nonlinear refractive index. In InSb, their calculation suggests a self-focusing action even much stronger than in CS_2. No experiment has yet been performed to verify their predictions. Borsheh and Brodin[91] have observed self-focusing in CdS, but have not been able to resolve the physical mechanism responsible for self-focusing.

Laser engineers who design high-power laser amplifiers have long been aware of the importance of eliminating self-focusing in order to avoid damage to the laser rods. Quantitative study of self-focusing in an amplifying medium has however been rare. Recently, Fleck and Layne[92] have made a simple numerical calculation on such a problem. Their results seem to agree quite well with the experimental observation.

VI Self-Focusing of Picosecond Pulses and Transient Self-Focusing in Kerr Liquids.

A large number of self-focusing experiments has been done on various liquids [39-41,43,45-47] and solids[39,43,44] with picosecond pulses. In almost all the experiments, emphasis is on the study of "small-scale filaments". The general characteristics of these filaments are quite similar to those observed with nanosecond pulses : they are a few microns in diameter, somewhat smaller than in the

nanosecond case, and a few cm in length; the light emitted from a filament often shows exceedingly large spectral broadening, occasionally larger than the fundamental vibrational frequency of the medium.

Unlike the nanosecond case, the experiments with picosecond pulses have usually been done with multimode lasers. Many, or at least several, filaments appear on each shot. Because of experimental difficulties, the characteristics of the input picosecond pulses are never carefully measured. As we have seen in Sec. IV, some characteristics of the filaments, such as spectral broadening, depend critically on the input conditions. This statement would presumably also apply to the present case. Therefore, quantitative analysis of the experimental results becomes rather impossible.

Most of the experiments were on Kerr liquids.[39-41,45,46] The results of Svelto and co-workers[40,45] are probably most well presented and have been most carefully analyzed. Instead of a train of mode-locked pulses, Reintjes et al[46] used a single picosecond pulse in the self-focusing experiment. This avoids complication arising from residual effects induced in the medium by the preceeding pulses in the train. Their results are similar to those of Svelto et al. These experiments give the following filament characteristics.

1) The filaments have a characteristic diameter of a few microns in a given medium, and have an approximate Gaussian intensity

profile.[39]

2) The side-view pictures show that the filaments are usually few cm long. They do not necessarily terminate at the exit window.

3) Radiation from the filaments show extensive spectral broadening with semiperiodic structure. In some cases, broadenings on Stokes and anti-Stokes sides are nearly equal (See Fig.20).

4) Spectral broadening appears to have no radial dependence over the cross-section of a filament.

5) Spectral broadening increases with the input peak power and the cell length.

Svelto et al[40,45] have used the self-trapping model to explain these results. For successful interpretation, they have to assume a physical mechanism (rocking of molecules) that contributes non-negligibly to Δn and has a relaxation time in the sub-picosecond range.[40] They have also arrived at the unreasonable conclusion that Δn must have the form $\Delta n = \Delta n_1(r) + \Delta n_2(z,t)$ where the time-independent $\Delta n_1(r)$ which depends only on the radial co-ordinate is responsible for trapping and the time-dependent $\Delta n_2(z,t)$ which depends on the field intensity is responsible for phase modulation and spectral broadening.[45] We now know that a picosecond pulse can self-focus into a dynamic trapping state.[48,50] The above-mentioned experimental observations can be well explained by the dynamic trapping model (which can also be considered as a modified moving focus model[36,50] as we shall see). The assumptions used by Svelto et al. in their interpretation can be avoided.

The difference between self-focusing of a nanosecond pulse and self-focusing of a picosecond pulse in an ordinary Kerr liquid is in the

fact that while the pulsewidth is much longer than the relaxation time τ of the Kerr effect in the former case, it is comparable or shorter in the latter case. Consequently, for self-focusing of a picosecond pulse in Kerr liquids the quasi-steady-state theory no longer holds, and the entire self-focusing process is a transient phenomenon. The self-focusing dynamics is then only correctly described by the solution of Eq. (1) coupled with the relaxation equation for Δn

$$\left(\frac{\partial}{\partial t} + \frac{1}{\tau}\right)\Delta n = \frac{1}{\tau}\,\Delta n_o(|E|^2). \tag{16}$$

Akhmanov et al[48] have considered an approximate analytical solution of the problem. Fleck and Kelley[49] did the numerical calculation. More recently, Shimizu and Courtens[50] and Fleck and Casman[51] have repeated the numerical calculation with a finer mesh.

Let us first give a qualitative description of the solution one would expect from physical reasoning. Since the input pulse is short, the response of Δn to the pulse never reaches the steady state. From Eq. (16), we can write

$$\Delta n(z,\xi) = \left(\frac{1}{\tau}\right) \int_{-\infty}^{\xi} \Delta n_o(|E(z,\eta)|^2)\, \exp[-(\xi-\eta)/\tau]\, d\eta \tag{17}$$

where $\xi = t - zn_o/c$. It is then clear that if the pulsewidth is comparable to the relaxation time τ, the later part of the pulse may see a larger Δn than the former part. Consequently, different parts of the pulse will propagate in the medium differently as sketched in Fig. 21. The very first part (a in the figure) of the pulse sees little induced Δn and diffracts almost linearly as it propagates in the medium. The next part (b in the figure) of the pulse sees somewhat larger Δn, but not large enough to cause self-focusing; and therefore it still diffracts but not as strongly. Then, Δn induced by the front part is large enough to cause the

middle part (c-f in the figure) to self-focus.

However, as the beam propagates on, it sees a gradually decreasing Δn because the front part of the pulse has diffracted in the medium. The middle part of the pulse then self-focuses first and eventually diffract. Both self-focusing and diffraction are very gradual, leading to a long focus. The minimum diameter of the focus depends on how large a Δn it sees. The later part of the pulse may see a larger Δn and therefore tends to self-focus earlier to a smaller minimum diameter, but the diffraction is still slow since the front part of the pulse diffracts rather slowly. It is likely that the minimum diameter is limited by some other highly nonlinear process. When this happens, we may find that the minimum diameter reached by self-focusing is the same for a finite section of the pulse.

The above picture shows that we can still talk about moving focus if we define the position of the focus as the position where the minimum diameter occurs. Aleshkevich et al[48] have discussed the problem in terms of a moving focus. However, we see from Fig. 21 that it is not really appropriate to talk about moving focus in this case : the longitudinal dimension of the focus (a few cm) is much longer than even the pulse length ($\lesssim$ 1 mm); the transverse dimension of the focus varies markedly as the focus moves along the axis; the corresponding field intensity at the focus also varies appreciably as the focus moves. In fact, the field intensity at a local point is not necessarily a maximum when the focus arrives at that point. This picture is therefore quite different from the moving focus picture we discussed in Sec. III for the case of quasi-steady-state self-focusing, but the differences are really only in the focal dimensions and in the detailed geometry of focusing and defocusing.

Knowing how the various parts of the pulse propagate in the medium, we

have immediately the picture of how the transverse profile of the pulse gets deformed. This is also sketched in Fig. 21. Upon self-focusing, the middle part of the pulse shrinks in diameter as it propagates, so that the pulse is quickly deformed into a horn shape. Because of the slow focusing and diffraction, the horn-shape pulse soon appears to have reached a stable state of deformation and can then propagate on for many cm without appreciable change in its shape (See Fig. 21). This stable form of propagation of the pulse has received the name of dynamic trapping,[93] in order to be distinguished from the self-trapping picture originally suggested by Chiao et al[1]. It is then clear that the neck part of the horn sweeping along the axis leads to the observed filament, and the diameter of the filament corresponds to the diameter of the neck. The filament finally disappears when the transverse profile of the entire pulse expands through diffraction. This could happen inside the cell if the cell is sufficiently long.

The spectral broadening of light can also be understood from the above picture.[36, 50] Since the various parts of the pulse see different Δn along their paths in the medium, the phase increments $\Delta\phi$ (or ks in Eq. (2b)) they acquire along the paths also vary. This means phase modulation, and hence spectral broadening of the light pulse. As a first crude approximation, we neglect the phase increment acquired by the pulse before the pulse reaches the more or less stable horn shape. Assuming a given intensity distribution in the horn-shape pulse which propagates for a distance z to the end of the cell without change of shape, we can then find the phase modulation of light emitted from the axial region at the end of the cell. The corresponding broadened spectrum can then be obtained by Fourier transform. An example is shown in Fig. 22.[36] The spectrum has indeed the semiperiodic structure with Stokes and anti-Stokes broadening nearly equal; the extent of broadening is proportional to z. The anti-

Stokes broadening here comes from the neck region of the pulse. The fast reduction of the radius of the pulse close to the neck region increases the diffractive contribution Δn_{eff} in Eq. (10), and consequently, Δn_{eff} and $\Delta\phi(t)$ decrease with time. The large negative slope on the lagging part of the $\Delta\phi(t)$ curve then gives rise to appreciable anti-Stokes broadening. The more or less symmetric curve of $\Delta\phi(t)$ is responsible for the nearly symmetric Stokes and anti-Stokes broadening. In general, the $\Delta\phi(t)$ curve is of course not necessarily symmetric, depending on the detail of the horn shape. More rigorously, propagation of the pulse in the region before the pulse turns into the stable horn shape may also affect the $\Delta\phi(t)$ curve appreciably.

Shimizu[50] has confirmed the above picture by the numerical solution of Eqs. (1) and (16). He has also calculated the spectral broadening under various conditions. The semi periodic structure of the broadened spectrum is indeed nearly independent of the radial coordinate over the cross-section of the filament. Fleck and Carman[51] have obtained similar results. The experimental observations on self-focusing of picosecond pulses in Kerr liquids are therefore qualitatively explained.

Shimizu's calculation[50] however indicates that the filament diameter depends critically on the peak power of the input picosecond pulse; a higher input power gives a thinner filament. Experimental results show no dependence of the filament diameter on input power. It is therefore suspected that some highly nonlinear optical process is responsible in limiting the filament diameter. Various possibilities were discussed in Sec. IV F. Yablonovitch and Bloembergen[57] have suggested that the pre-breakdown avalanche ionization is perhaps the limiting mechanism. Their estimates appear to be in reasonable agreement with the measurements of Brewer and Lee[39]. Shimizu[50] has considered various nonlinear

saturation and absorption mechanisms including stimulated Raman scattering in his self-focusing calculation. The results are, however, rather complicated.

In order to have a better understanding of transient self-focusing in Kerr liquids, we need more quantitative experimental results. It would be ideal if in the experiment, the input conditions can be measured accurately, the stimulated Raman and Brillouin scattering and other nonlinear optical processes can be suppressed, and the input pulsewidth relative to the relaxation time can be varied. Such an experiment has recently been carried out by Wong and Shen.[53] They use an isotropic liquid crystalline material as the nonlinear medium. Because of pretransitional behavior, such materials have large field-induced refractive indices and slow orientational relaxation times which vary with temperature.[52] For the nematic substance MBBA, the relaxation time τ varies from 40 nsec to 1 μsec. It then becomes possible to use a Q-switched laser pulse to study transient self-focusing in such a Kerr liquid. The results of Wong and Shen[53] prove conclusively the dynamic trapping model. In their case, stimulated Raman and Brillouin scattering do not appear to interfere with self-focusing. The laser intensity in the focal region is also not strong enough to cause breakdown. It is believed that multiphoton absorption is probably the mechanism responsible for the limiting diameter. However, since $\partial(\Delta n)/\partial t$ or the phase modulation induced by a Q-switched pulse is small, no appreciable spectral broadening can be observed in this case.

Self-focusing of picosecond pulses and the resulting small-scale filaments with large spectral broadening have also been observed in non-Kerr liquids,[94] rare-gas liquids,[43,47] glasses,[39,42] and crystals.[42,44] In these media, molecular libration, reorientation, and redistribution have presumably negligible contribution to Δn. Electrostriction is too slow to respond to a picosecond pulse (in this respect, a clean experiment should use a single pulse instead of a train of pulses.)

Electronic nonlinearity is believed to be the only dominant mechanism for the observed Δn. The corresponding relaxation for Δn is therefore of the order of 10^{-15} sec. One expects that the quasi-steady-state theory of self-focusing and the moving focus model are valid in this case. As shown in Secs. III and IV, the moving focus should yield a filament pulse (light pulse emitted from the filament at the exit face of the medium) with a pulsewidth of a few relaxation times. Then, in the present case, we would expect to find a filament pulse as short as $\sim 10^{-14}$ sec. This would be the shortest optical pulse ever generated in experiments. The actual pulsewidth measurement on such a filament pulse has not yet been carried out. The presently available photo-detection system is still not fast enough to have the necessary time resolution. Spectral broadening of the filament pulse can, however, be measured quite accurately. In most cases, the broadened spectrum shows only weak or no semi-periodic structure.[43,47] This is what one would expect if the observed spectral broadening is not dominated by phase modulation but by the inverse of the pulsewidth. A 5×10^{-15} sec. smooth pulse with no phase modulation would lead to a 1000 cm^{-1} spectral broadening with no fine structure. Bloembergen[95] has recently suggested that the anomalously large antiStokes spectral broadening could be due to plasma formation during prebreakdown. The sudden increase in the free electron density through ionization leads to a sudden drop in Δn. The large negative rate of change of Δn is then responsible for the huge antiStokes broadening. Penkover *et al.*[96] have, however, proposed that in non-Kerr liquids, this superbroadening may be the results of stimulated Stokes-antiStokes scattering[97,98] (or stimulated parametric scattering). Because of the high intensity of the picosecond laser pulse, saturation and higher-order stimulated scattering can occur and lead to the anomalously large spectral broadening. Most interpretations of the results on filaments in rare-gas liquids and solids in the literature have been based on the

self-trapping model. We can now see that such interpretations are perhaps incorrect. but in order to be sure that the moving focus model is correct, we still need more carefully measured experimental data. The problem is clearly a very interesting one and is definitely worth pursuing.

VII. Other Self-Focusing Effects

We shall briefly discuss in this section several other self-focusing phenomena which have been observed.

Most of the self-focusing experiments have been done on liquids and solids, but self-focusing in gases has also been reported.[59] Using a Raman-shifted ruby-laser beam (peak power, 1.5 kW; pulsewidth, 5 nsec; diameter, 1 mm) at several cm^{-1} above

the 7665-Å line of potassium in a 100 - cm potassium vapor cell, Grischkowsky[59] has observed clear self-focusing of the beam when the density of the vapor is sufficiently high. The minimum diameter of the self-focused beam detected was about 50 μm. The focal region appeared to extend along the axis for many centimeters. No other nonlinear optical processes such as stimulated scattering were observed in the experiment. In this case, the nonlinear refractive index necessary for self-focusing arises from the intensity-dependent anomalous dispersion of the refractive index.[59,60]

$$\Delta n = \frac{A}{\omega-\omega_o} [1-(1 + |E|^2/E_s^2)^{-1}]$$

where A is a positive constant, ω_o is the resonant frequency, and E_s proportional to $(\omega - \omega_o)$ is defined as the saturation field. For $\omega > \omega_o$, we find a positive Δn which increases with the field and causes the beam to self-focus. From the theoretical point of view the problem is most attractive, since no other nonlinear process is present to complicate the self-focusing process and Δn which responds instantaneously to the field is well defined up to very high field strength. Thus, a complete solution of the problem can be worked out to compare with the experimental results.[61] For $\omega < \omega_o$, Δn is negative and the beam should self-defocus. This is indeed what Grischkowsky has observed.[59,99] The results agree well with the theoretical calculation.[99]

Spectral broadening associated with self-focusing and self-defocusing in alkali vapor has also been observed.[100,101] Arutunian et

al.[100] and Akhmanov et al[102] used the simple theory of phase modulation proposed by Shimizu[79] and others[80,83] to explain the observed spectral broadening. A correct description of amplitude and phase modulation on the output pulse should however be obtained from the complete self-focusing (or self-defocusing) solution. This subject has not been throughly investigated yet.

Thermal self-focusing is a different self-focusing problem which is well understood. The effect has so far only been observed in solids.[103-112] The threshold power for observing thermal self-focusing is generally low (0.1 - 10 W). The nonlinearity arises from heating of the medium through absorption of the laser beam.[110-114]

$$\Delta n = \frac{\partial n}{\partial T} \Delta T$$

$$= \left(\frac{\partial n}{\partial T}\right)_\rho \Delta T + \left(\frac{\partial n}{\partial \rho}\right)_T \left(\frac{\partial \rho}{\partial T}\right) \Delta T \qquad (18)$$

where $(\partial n/\partial T)_\rho$ can be positive if the absorption bands of the medium shift with increasing temperature in such a way that the refractive index Δn increases, and $(\partial n/\partial \rho)_T (\partial \rho/\partial T)$ is always negative because the thermal expansion $(\partial \rho/\partial T)$ is negative. In some media, the resultant $(\partial n/\partial T)$ is positive, but in others, $(\partial n/\partial T)$ is negative. However, if a laser pulse is used, the thermal effect may never reach equilibrium during the pulse. Even if the steady state $(\partial n/\partial T)$ is less than zero, the transient $(\partial n/\partial T)$ can be positive when the density variation which propagates with sound velocity is still in the transient state.[111] Relaxation among various energy states may also play a role in delaying thermalization of the system. The positive Δn

either steady state or transient, can then lead to thermal self-focusing.

Both steady-state[103-107] and transient[106,108-112] thermal self-focusing have been observed. Akhmanov et al.[103] first reported the observation of steady-state thermal self-focusing in $LiNbO_3$ doped with Nd. Dabby and Whinnery[105] studied steady-state thermal self-focusing in lead glass. They found that at least part of the self-focused beam can tunnel into a trapped filament in this case (see Fig. 23). Nonlinear spherical aberration in self-focusing was seen. Dabby et al.[108] can Carman et al.[106] used pulsed lasers to study transient thermal self-focusing in lead glass and Nd doped glass. They showed that the self-focusing distance indeed varied with time and the output pulse had a frequency modulation as predicted by theory. These experiments were all carried out by an argon laser. Zverev et al.[109-111] and Karlor et al.[112] found with a pulsed solid-state laser that thermal self-focusing was probably connected with the damage of an absorbing solid. Thermal self-defocusing in various media have also been extensively studied, but we shall not discuss the problem here.[3,113,114]

Bjorkholm and Ashkin[115] have recently observed steady-state self-focusing in potassium vapor with a tunable cw dye laser. Under suitable conditions, the self-focused beam can also tunnel into a trapped filament. This case is probably quite similar to the case of steady-state thermal self-focusing. Here, instead of thermal diffusion, energy can diffuse out of the focal region via resonant fluorescence and atomic collision.

Self-focusing in air in the breakdown region has also been reported.[116] It is presumably responsible for the backward propagation of the breakdown spot. A quantitative study of this phenomenon appears to be rather difficult.

VIII Conclusion.

We have seen that the phenomenon of self-focusing in various media is now fairly well understood, at least in a qualitative way. A

few problems, such as the filament diameter, the self-focusing dynamics in the focal region, transient self-focusing in different media, etc., still remain to be solved. Further progress in this field however requires more quantitative results from both theoretical and experimental investigation. How self-focusing would affect the various nonlinear optical processes in a medium was originally the motivation for studying self-focusing. The answer to the question has nevertheless been impeded by the complexity of the self-focusing phenomenon. Now that we have achieved a fair understanding on self-focusing, the time is perhaps ripe for us to go back to consider this question seriously again.

ACKNOWLEDGEMENT

Supported in part by the U. S. Atomic Energy Commission through the Inorganic Materials Research Division, Lawrence Berkeley Laboratory, Berkeley, California 94720.

References

1. R.Y. Chiao, E. Garmire, and C.H. Townes, Phys. Rev. Lett. 13, 479 (1964); (Erratum, Phys.Rev.Lett. 14, 1056 (1965)).

2. E.L. Kerr, Phys.Rev. A4, 1195 (1971).

3. S.A. Akhmanov, R.V. Khokhlov, and A.P. Sukhorukov, in "Laser Handbook", edited by F.T. Arecchi and E.O. Schulz-Dubois, (North-Holland Publishing Co., Amsterdam, 1972) p.1151.

4. O. Svelto, in "Progress in Optics," Vol.XII,

5. M. Hercher, J.Opt. Soc. Am. 54, 563 (1964).

6. G.A. Askar'yan, Zh: Eksp. Teor. Fiz. 42, 1567; 42, 1672 (1962); English Translation : Sov. Phys. JETP 15, 1088; 15, 1161 (1962) .

7. V.I. Talanov, Izv. Vuzov (Radiofizika) 7, 564 (1964).

8. E.J. Woodbury and W.K. Ng, Proc.IRE 50, 2367 (1962); M.Geller, D.P.Bortfeld, and W.R. Sooy, Appl. Phys. Lett. 3, 36 (1963); E.Eckhardt, D.P. Bortfeld, and M.Geller, Appl. Phys. Lett. 3, 136 (1963); B.P. Stoicheff, Phys.Lett. 7, 186 (1963); R.W. Minck, R.W. Terhune, and W.G. Rado, Appl. Phys. Lett. 3, 181 (1963).

9. E. Garmire, Phys.Lett. 17, 251 (1965); Ph.D. Thesis, Mass. Inst. of Technology, (1966).

10. R.W. Hellwarth, Phys.Rev. 130, 1850 (1963); Appl.Optics 2, 847 (1963); E. Garmire, F. Pandarese, and C.H. Townes, Phys.Rev.Lett. 11, 160 (1963); N. Bloembergen and Y.R. Shen, Phys. Rev.Lett. 13, 720 (1964); Phys. Rev. 133, A37 (1964); Y.R. Shen and N.Bloembergen, Phys.Rev.137, A1786 (1965);

11. Y.R. Shen and Y.J. Shaham, Phys.Rev.Lett. 15, 1008 (1965); P. Lallemand and N.Bloembergen, Phys.Rev.Lett.15, 1010 (1965); G.Hanchecorne and G. Mayer, Compt. Rend. 261, 4014 (1965); N.F. Pilipetskii and A.R. Rustamov, ZhETF Pis'ma 2, 88 (1965) English Translation : JETP Lett. 2, 55 (1965) .

12. V.I. Talanov, ZhETF Pis'ma 2, 218 (1965) English Translation : JETP Lett. 2, 138 (1965) .

13. P.L. Kelley, Phys.Rev.Lett. 15, 1005 (1965) Erratum : Phys. Rev. Lett. 16, 384 (1966) .

14. C.C. Wang, Phys. Rev. Lett. 16, 344 (1966); Phys. Rev. 152, 149 (1966), J.Appl. Phys. 37, 1943 (1966); C.C. Wang and G.W. Racette, Appl. Phys. Lett. 8, 256 (1966).

15. E. Garmire, R.Y. Chiao, and C.H. Townes, Phys. Rev. Lett. 16, 347 (1966)

16. R.Y. Chiao, M.A. Johnson, S. Krinsky, H.A. Smith, C.H. Townes, and E. Garmire, IEEE J. Quant. Electron. QE-2, 467 (1966).

17. R.G. Brewer and J.R. Lifsitz, Phys. Lett. 23, 79 (1966).

18. R.G. Brewer and C.H. Townes, Phys. Rev. Lett. 18, 196 (1967).

19. R.G. Brewer, J.R. Lifsitz, E. Garmire, R.Y. Chiao, and C.H. Townes, Phys. Rev. 166, 326 (1968).

20. Y.R. Shen, M.Y. Au Yang, and M.L. Cohen, Phys. Rev. Lett. 19, 1171 (1967); K. Grob and M. Wagner, Phys. Rev. Lett. 17, 819 (1966).

21. M.M.T. Loy and Y.R. Shen, Phys. Rev. Lett. 22, 994 (1969).

22. S.A. Akhmanov, A.P. Sukhorukov, and R.V. Khokhlov, ZhETF 50, 1537 (1966); English Translation : Sov. Phys. JETP 23, 1025 (1966).

23. G. McAllister, J. Marburger, and L. Dé Shazer, Phys. Rev. Lett. 21, 1648 (1968).

24. M. Maier, G. Wendl, and W. Kaiser, Phys. Rev. Lett. 24, 352 (1970); M. Maier, O. Rehn, and G. Windl, Z. Naturforsh, A25, 1868 (1970).

25. See the following article on the theoretical aspects of self-focusing by J. Marburger.

26. V.N. Goldberg, V.I. Talanov, and R.E. Irm, Izv. Vysshikh Uchebn. Zavedenii, Radiofizika 10, 674 (1967).

27. J.H. Marburger and E.L. Dawes, Phys. Rev. Lett. 21, 556 (1968); E.L. Dawes and J.H. Marburger, Phys. Rev. 179, 862 (1969).

28. J.H. Marburger and W.G. Wagner, IEEE J. Quant. Electron. (Corresp.) QE-3, 415 (1967).

29. V.N. Lugovoi and A.M. Prokhorov, ZLETF Pis'ma 7, 153 (1968), English Translation, JETP Lett. 7, 117 (1968); A.L. Dyshko, V.N. Lugovoi, and A.M. Prokhorov, ZLETF Pis'ma 6, 655 (1967), English Translation : JETP Lett. 6, 146 (1967) ; V.N. Lugovoi, Doklady Akademii Nauk SSSR 176, 58 (1967) English Translation : Sov. Phys. Doklady 12, 866 (1968).

30. J.P. Taran and T.K. Gustafson, IEEE J. Quant. Electron. (Corresp.) QE-5, 381 (1969).

31. M.M.T. Loy and Y.R. Shen, Phys. Rev. Lett. 25, 1333 (1970).

32. M.M.T. Loy and Y.R. Shen, Appl. Phys. Lett. 19, 285 (1971).

33. G.M. Zverev, E.K. Maldutis, and V.A. Pashkov, ZhETF Pis'ma 9, 108 (1969) English Translation : JETP Lett. 9, 61 (1969) ; G.M. Zverev and V.A. Pashkov, Zh. Eksp. Teor. Fiz. 57, 1128 (1969) English Translation : Sov. Phys. JETP 30, 616 (1970).

34. V.V. Korobkin, A.M. Prokhorov, R.V. Serov, and M. Ya. Shchelev, ZhETF Pis'ma 11, 153 (1970) English Translation : JETP Lett. 11, 94 (1970) .

35. Y.R. Shen and M.M.T. Loy, Phys. Rev. A3, 2099 (1971).

36. M.M.T. Loy and Y.R. Shen, IEEE J. Quant. Electron. QE-9, 409 (1973).

37. N.I. Lipator, A.A. Manenkov, and A.M. Prokhorov, ZhETF Pis'ma 11 , 444 (1970); English Translation : JETP Lett. 11 , 300 (1970) .

38. C.R. Giuliano and J.H. Marburger, Phys. Rev. Lett. 27, 905 (1971).

39. R.G. Brewer and C.H. Lee, Phys. Rev. Lett. 21 , 267 (1968).

40. R. Polloni, C.A. Sacchi, and O. Svelto, Phys. Rev. Lett. 23, 690 (1969); R. Cubeddu, R. Polloni, C.A. Sacchi, and O. Svelto, Phys. Rev. A2 , 1955 (1970).

41. M.A. Bol'shov, G.V. Vinkin, S.A. Zhilkin, and J.J. Nurmininskii, ZhETF 58, 3 (1970); English Translation : Sov. Phys. JETP 31, 1 (1970) .

42. R.R. Alfano and S.L. Shapiro, Phys. Rev. Lett. 24, 592 (1970).

43. R.R. Alfano and S.L. Shapiro, Phys. Rev. Lett. 24, 1217 (1970)

44. N.G. Bondarenko, I.V. Eremina, and V.V. Talanov, ZhETF Pis'ma 12, 125 (1970); English Translation : JETP Lett. 12, 85 (1970) .

45. R. Cubaddu, R. Polloni, C.A. Sacchi, O. Svelto, and F.Zagara, Phys. Rev. Lett. 26, 1009 (1971); R. Cubeddu and F.Zagara, Opt. Comm. 3 , 310 (1971).

46. J. Reintjes, R. L. Carman, and F. Shimizu, Phys. Rev. A8, 1486 (1973). R. Reintjes, Ph.D. Thesis, Harvard University, 1972.

47. J.P. McTague, C.H. Lin, T.K. Gustafson, and R.Y. Chiao, Phys. Lett. 32A, 82 (1970).

48. S.A. Akhmanov, A.P. Sukhorukov, and R.V. Khokhlov, ZhTEF, 51, 296 (1966) JETP 24, 198 (1966) ; V.A. Alashkevich, S.A. Akhmanov; A.P. Sukhorukov, and A.M. Khachatryan, ZhTEF Pis'ma 13, 55 (1971) English Translation : JETP Lett. 13, 36 (1971) .

49. J.A. Fleck and P.L. Kelley, Appl. Phys. Lett. 15, 313 (1969).

50. F. Shimizu, IBM Report RZ538 (1972); F. Shimizu and E. Courtens, paper presented at the Isfahan Symposium on Fundamental and Applied Laser Physics, Isfahan, Iran. (Aug. 1971).

51. R.L. Carman and J.A. Fleck, Appl.Phys.Lett. 20, 290 (1972)

52. G. K. L. Wong and Y. R. Shen, Phys. Rev. Lett. 30, 895 (1973).

53. G. K. L. Wong and Y. R. Shen, Phys. Rev. Lett. 32, 527 (1973).

54. A.L. Dyshko, V.N. Lugovoi, A.M. Prokhorov, ZhTEF 61, 2305 (1971); English Translation : Sov. Phys. JETP 34, 1235 (1972) .

55. O. Rehn and M. Maier, Phys. Rev. Lett. 29, 558 (1972); Phys. Rev. (to be published).

56. P.L. Kelley and T.K. Gustafson, Phys. Rev. A8, 315 (1973).

57. E. Yablonovitch and N. Bloembergen, Phys. Rev. Lett. 29, 907 (1972).

58. T.K. Gustafson and C.H. Townes, Phys. Rev. A6 , 1659 (1972).

59. D. Grischkowsky, Phys. Rev. Lett. 24, 866 (1970).

60. A. Javan and P.L. Kelley, IEEE J. Quant. Electron. QE-2, 470 (1966)

61. M.M.T. Loy and D. Grischkowsky (Private Communications).

62. See for example, S.A. Akhmanov, A.P. Sukhorukov, and

62. (cont) R.V. Khokhlov, Usp. Fiz. Nauk. 93, 19 (1967) Soviet Physics Uspekhi 93, 609 (1968) .

63. W.G. Wagner, H.A. Haus, and J.H. Marburger, Phys.Rev. 175, 256, (1968).

64. S.K. Akhmanov, A.P. Sukhorukov, and R.V. Khokhlov, ZhETF 50 1537 (1966) English Translation : Soviet Physics JETP 23, 1025 (1966) .

65. V.E. Zakharov, V.V. Sobolev, and V.S. Synakh, ZhETF 60, 136 (1971). English Translation : Sov. Phys. JETP 33, 77 (1971) .

66. G.K.L. Wong and Y.R. Shen, (to be published).

67. E.L. Kerr, Phys. Rev. A6, 1162 (1972).

68. V.I. Bespalov and V.I. Talanov, ZhETF Pis'ma 3, 471 (1966), English Translation : JETP Letters 3, 307 (1966) .

69. R. Y. Chiao, P. L. Kelley, and E. Garmire, Phys. Rev. Lett. 17, 1158 (1966).

70. R. L. Carman, R. Y. Chiao, and P. L. Kelley, Phys. Rev. Lett. 17, 1281 (1966).

71. A. J. Campillo, S. L. Shapiro, and B. R. Suydam, Appl. Phys. Lett. 23, 628 (1973); ibid., 24, 178 (1974).

72. S.C. Abbi and H. Mahr, Phys. Rev. Lett. 26, 604 (1971); Appl. Phys. Lett. 19, 415 (1971).

73. D.H. Close, C.R. Giuliano, R.W. Hellwarth, L.D. Hess, F.J. McClung, and W.G. Wagner, IEEE J. Quant. Electron. QE-2, 553 (1966).

74. F. Shimizu and B.P. Stoicheff, IEEE J. Quant. Electron. 5, 544 (1969).

75. D.J. Bradley, B. Libby, W. Sibbett, and W.E. Sleat, Appl. Phys. Lett. 20, 219 (1972).

76. M. Maier, W. Kaiser, and J.A. Giordmaine, Phys. Rev. Lett. 17, 1275 (1966); Phys. Rev. 177, 580 (1969).

77. Y.R. Shen and Y.J. Shaham, Phys. Rev. 163, 224 (1967).

78. R.G. Brewer, Phys. Rev. Lett. 19, 8 (1967).

79. F. Shimizu, Phys. Rev. Lett. 19, 1097 (1967).

80. A.C. Cheung, D.M. Rank, R.Y. Chiao, and C.H. Townes, Phys. Rev. Lett. 20, 786 (1968).

81. J.R. Lifsitz and H.P.H. Grieneisen, Appl.Phys. Lett. 13, 245 (1968).

82. M. M. Denariez-Roberge and J-P. E. Taran, Appl. Phys. Lett. 14, 205 (1969).

83. T. K. Gustafson, J-P. E. Taran, H. A. Haus, J. R. Lifsitz, and P. L. Kelley, Phys. Rev. 177, 306 (1969).

84. G. K. L. Wong and Y. R. Shen, Appl. Phys. Lett. 21, 163 (1972).

85. T. K. Gustafson, P. L. Kelley, R. Y. Chiao, and R. G. Brewer, Appl. Phys. Lett. 12, 165 (1968).

86. J. Marburger, L. Huff, J. D. Reichert, and W. G. Wagner, Phys. Rev. 184, 255 (1969).

87. N. Bloembergen, (to be published).

88. G. N. Steinberg, Phys. Rev. 4A, 1182 (1971).

89. Y. R. Shen, Phys. Lett. 20, 378 (1966).

90. N. Tzoar and J. L. Gersten, Phys. Rev. Lett. 26, 1634 (1971); Phys. Rev. B4, 3540 (1971).

91. A. A. Borshch and M. S. Brodin, ZhETF 58, 26 (1970); English translation: Soviet Phys. JETP 31, 15 (1970); I. V. Baranovskii, A. A. Borsch, M. S. Brodin, and A. M. Kamuz, ZhETF 60, 1593 (1971); English translation: Sov. Phys. JETP 33, 861 (1971).

92. J. A. Fleck and C. Layne, Appl. Phys. Lett. 22, 467 (1973).

93. N. Bloembergen, paper presented at the Ishahan Symposium on Fundamental and Applied Laser Physics, Isfahan, Iran, August 1971.

94. D. L. Weinberg, Appl. Phys. Lett. 14, 32 (1969); W. Werncke, A. Lau, M. Pfeiffer, K. Lenz, H. J. Weigmann, and C. D. Thuy, Opt. Comm. 4, 413 (1972); V. S. Dneprovsky, K. V. Karmenjan, and I. I. Nurminsky, Izv. Akad. Nauk Arm. SSR, Fiz. 7, 348 (1972).

95. N. Bloembergen, Optics Comm. (to be published).

96. A. Penzkofer, A. Laubereau, and W. Kaiser, Phys. Rev. Lett. 31, 863 (1973).

97. Y. R. Shen and N. Bloembergen, Phys. Rev. 137, A1787 (1965).

98. R. R. Alfano and S. L. Shapiro, Phys. Rev. Lett. 24, 584 (1970).

99. D. Grischkowsky and J. A. Armstrong, Phys. Rev. A6, 1566 (1972).

100. V. M. Arutunian, N. N. Badalyan, V. A. Iradyan, and M. E. Movsesyan, ZhETF 58, 37 (1970); English translation: JETP Lett. 31, 22 (1970).

101. S. Yu. Kirin, S. Rautian, A. Samenov, and B. Chernoborod, ZhETF Pis'ma 11, 340 (1970); English Translation: JETP Lett. 11, 226 (1970).

102. S. A. Akhmanov, A. I. Kovrygin, and V. Oglusdin, ZhETF Pis'ma 15, 186 (1972); English translation: JETP Lett. 15, 129 (1972).

103. S. A. Akhmanov and A. P. Sukhorukov, ZhETF Pis'ma 5, 109 (1967); English translation: JETP Lett. 5, 87 (1967).

104. S. A. Akhmanov, D. P. Krindach, A. V. Migulin, A. P. Sukhorukov, and R. V. Khokhlov, IEEE J. Quantum Electron. 4, 568 (1968).

105. F. W. Dabby and J. R. Whinnery, Appl. Phys. Lett. 13, 28 (1968).

106. R. L. Carman, A. Mooradian, P. L. Kelley, and A. Tufts, Appl. Phys. Lett. 14, 136 (1969).

107. S. A. Akhmanov, Yu A. Gorokhov, D. P. Krindach, A. P. Sukhorukov, and R. V. Khokhlov, ZhETF 57, 16 (1969); English translation: Sov. Phys. JETP 30, 9 (1969).

108. F. W. Dabby, T. K. Gustafson, J. R. Whinnery, Y. Kohanzadeh, and P. L. Kelley, Appl. Phys. Letters 16, 362 (1970).

109. G. M. Zverev, T. Ya. Mokhailova, V. A. Pashkov, and N. M. Soloviova ZhETF Pis'ma 5, 391 (1967); English Translation: JETP Letters 5, 319 (1967).

110. G. M. Zverev, E. A. Levchuk, E. K. Maldutis, ZhETF 58, 1487 (1970); English Translation: Sov. Phys. JETP 31, 794 (1970).

111. G. M. Zverev, E. A. Levchuk, E. K. Maldutis, and V. A. Pashkov, ZhETF Pis'ma 11, 177 (1970); English Translation: JETP Letters 11, 108 (1970).

112. N. V. Karlov, G. P. Kuzmin, and A. M. Prokhorov, ZhETF Pis'ma 12, 363 (1970); English Translation: JETP Letters 12, 248 (1970).

113. A. G. Litvak, ZhETF Pis'ma 4, 341 (1966); English Translation: JETP Letters 4, 230 (1966).

114. Yu P. Raizer, ZhETF Pis'ma 4, 286 (1966); ZhETF 52, 470 (1967); English Translation: JETP Letters 4, 85 (1966); JETP 25, 308 (1967).

115. J. E. Bjorkholm and A. Ashkin, Phys. Rev. Letters 32, 129 (1974).

116. V. V. Korobkin and A. J. Alcock, Phys. Rev. Letters 21, 1433 (1968); A. J. Alcock, C. De Michelis, V. V. Korobkin, and M. C. Richardson, Appl. Phys. Letters 14, 145 (1969); A. J. Alcock, C. De Michelis, and M. C. Richardson, IEEE J. Quantum Electron. 6, 622 (1970); L. C. Johnson and T. K. Chu, Phys. Rev. Letters 32, 517 (1974).

Figure Captions

Fig. 1. Image of small-scale filaments at the exit window of a CS_2 cell created by self-focusing of a multimode laser beam (after S.C. Abbi and H. Mahr, Ref. 67).

Fig. 2. Images of a self-focused single-mode laser beam at the exit window of a toluene cell of different cell lengths a) short cell length, beam not yet self-focused (~ 700 μm) b) cell length close to self-focusing threshold, the self-focused beam at nearly $^1/_{10}$ of its original size (~ 50 μm); c) cell length above the self-focusing threshold, the self-focused beam at its limiting size - the filament (10 μm).

Fig. 3. Sketch showing the distortion of the wavefront and self-focusing of a laser beam in a nonlinear medium.

Fig. 4. Square root of ratio of input power P to critical power P_{cr} versus inverse self-focusing length z_f. The dashed line is an asymptote of the curve at high powers, (after E.L. Dawes and J. Marburger, Ref. 27).

Fig. 5. Dependence of α in Eq. (6) on $(P/P_{cr})^{\frac{1}{2}}$ (after E.L. Dawes and J. Marburger, Ref. 27).

Fig. 6. Lower trace describes input power P(t) as a function of time t. Peak power is 42.5 kW and the half-width at the $^1/e$ point is 1 nsec. Upper trace, calculated from Eq. (5), describes the position of the focal spot as a function of time. Values of P_o and K used are 8 kW and 11.6 cm-$(kW)^{\frac{1}{2}}$ respectively, which corresponds roughly to an input beam of 400 um in diameter propagating in CS_2. The dotted lines, with the slope equal to the light velocity, indicate how light propagates in the medium along the z axis at various times. (After M.M.T. Loy and Y.R. Shen, Ref. 36).

Fig. 7. Normalized ratio of transmitted axial intensity I to the incident axial intensity I_o as a function of the ratio of the incident power P to the critical power P_c. The solid line represents the computer solution (focusing at the dotted line) and the circles represent the experimental data (After G.L. McAllister et al., Ref. 23).

Fig. 8. Sketch describing the interaction between backward stimulated scattering and incoming laser radiation. Backward stimulated Raman and Brillouin radiation, which is initiated along the upper branch of the U curve, propagates along the dot-dashed lines and interacts with the non-self-focused incoming laser light in the shaded region.

Fig. 9. Plot of the square root of threshold power for self-focusing in CS_2 as a function of the inverse cell length with both linearly and circularly polarized beams (after C.C. Wang Ref. 14).

Fig. 10. Time-of-flight experiment on the moving focal spot. The experimental set-up is shown on the left. The U curve on the right was obtained from Eq. (5) using experimentally determined parameters K , P_o , and P(t). The dots with error bars at 21 and 29.5 cm. are results obtained from the time-of-flight measurements with respect to the focal spot at the end of the 36-cm toluene cell. The dashed line with a slope equal to the light velocity is shown for comparison. (after M.M.T. Loy and Y.R. Shen, Ref. 36).

Fig. 11. (a) Schematic diagram showing the relative positions of the backward Raman pulse initiated at A and the filament pulse. Pulse separation at t_2 (when the focal spot reaches the exit window) is defined as d.

Fig. 11 (contd) (b) d as a function of input peak power for four different cell lengths. The solid curves are theoretical predictions calculated from the U curves determined by Eq. (5), using experimentally determined values of P_o and K (after M.M.T. Loy and Y.R. Shen, Ref. 32).

Fig. 12. Oscilloscope traces of the incident laser pulse (α), the total stimulated emission in the backward direction (β), the backward stimulated Raman emission alone (γ), and the transmitted laser light (δ). (After M.Maier et al., Ref. 71).

Fig. 13. Variation of Stokes and Brillouin power with laser power in 15-cm toluene at two different temperatures. (After Y.R. Shen and Y.J. Shaham, Ref. 72).

Fig. 14. Spectral broadening in a mixture of CS_2 and benzene. a) Experimental spectrum. (b) Theoretical fit obtained by assuming a Gaussian pulse of full $^1/e$ width of 5.4 psec and $k_o n_2 |E|^2 L/2n_o = 265$ in a self-trapped filament of length L. The relaxation time of the medium is assumed to be 9 psec. (After Gustafson et al., Ref. 78).

Fig. 15. A U curve describing the moving focus. The refractive index change Δn is appreciable in the shaded region which has a width of about a few relaxation times. Light traversing the cell along the dotted lines acquires a phase increment $\Delta\phi$ which varies with time t.

Fig. 16. Maximum Stokes broadening versus input peak power for given cell lengths. O — 15 cm of CS_2; Δ — 10 cm of CS_2; ∇ — 15 cm of toluene; $\square$ — 10 cm of toluene. The solid curves are calculated from Eq. (12) with an

Fig.16 (contd) input pulse of 1.2 nsec full width at $^1/e$ points, and with $(\Delta n_{eff})_{max} = (2.4 - .085) \times 10^{-3}$ for CS_2 and $(\Delta n_{eff})_{max} = (7 - .3) \times 10^{-4}$ for toluene. (After G.K.L. Wong and Y.R. Shen, Ref.79).

Fig.17. Theoretical power spectrum of the filament pulse obtained from the moving focus model for a 2 - nsec. input pulse described in Fig.6 propagating in a 22.5 - cm CS_2 cell. (After Y.R. Shen and M.M.T. Loy, Ref.35).

Fig.18. (a) Microdensitometer trace of a typical observed spectrum of light emitted from a filament, corresponding to a 10 - cm CS_2 cell and a 1.2 - nsec. input pulse with a peak power of 27 kW. (b) The calculated spectrum using the moving focus model. (After G.K.L. Wong and Y.R. Shen, Ref.79).

Fig.19. Typical example of (a) damage filament, (b) Streak photograph, and (c) oscilloscope trace for a temporarily smooth incident pulse (After C.R. Giuliano and J.H. Marburger, Ref.38).

Fig.20. Typical spectral broadening of filaments obtained with picosecond pulse excitation (After R.Polloni et al. Ref.40).

Fig.21. Sketch showing self-focusing of a picosecond pulse in a Kerr liquid. Different part (a, b, c, etc.) of the pulse focus and defocus along different ray paths. The pulse first gets deformed into a horn shape and then propagates on without much further change.

Fig. 22. Theoretical power spectrum obtained by assuming a horn-shape pulse propagating for a distance in a nonlinear medium without any change of its shape.

a) Normalized intensity of the output pulse versus time.

b) Field-induced phase increment $\Delta\phi$ in the filament ($\Delta\phi_{max}$ = 225 rad.)

c) Power spectrum of the filament output (after M.M.T. Loy and Y.R. Shen, Ref. 26).

Fig. 23. Thermal self-focusing of an argon laser beam inside a lead glass rod (ℓ = 35 cm) with input power a) P_o = 3 W, and b) P_o = 8 W. Part of the self-focused beam tunnels into a trapped filament (after F.W. Dabby and J.R. Whinnery, Ref. 95).

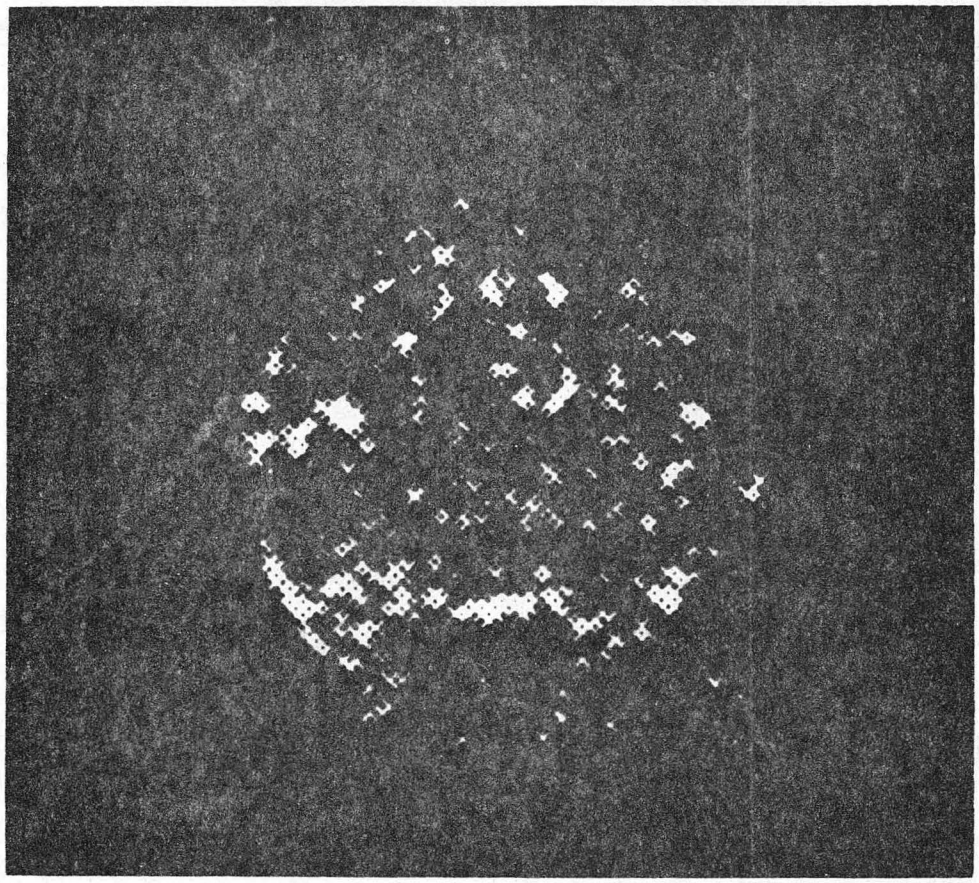

Fig. 1

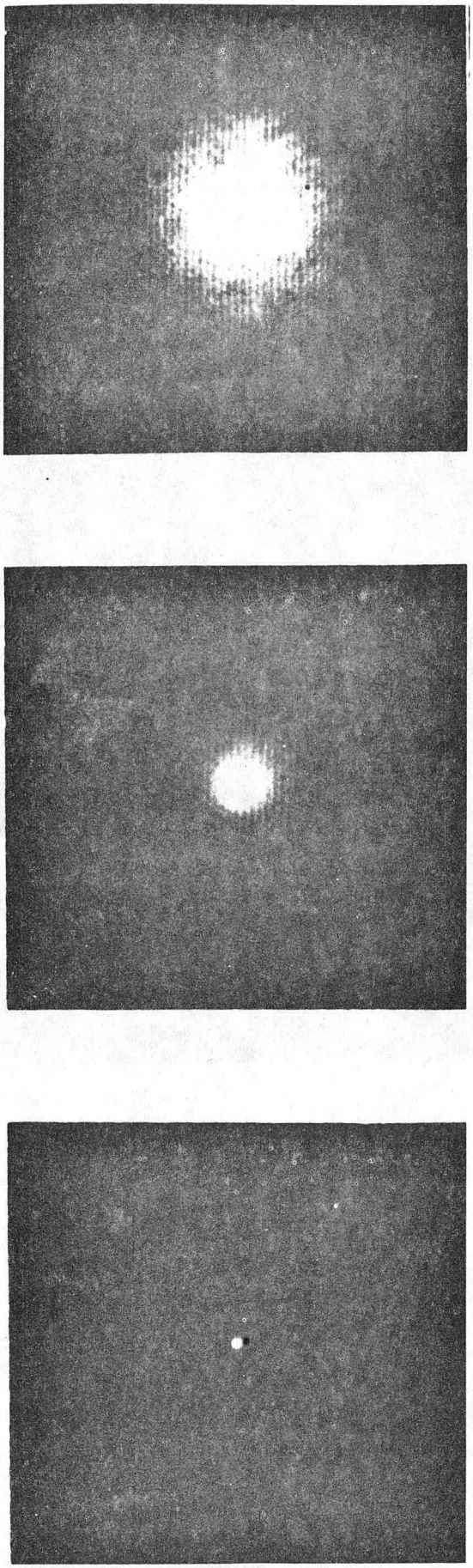

Fig. 2

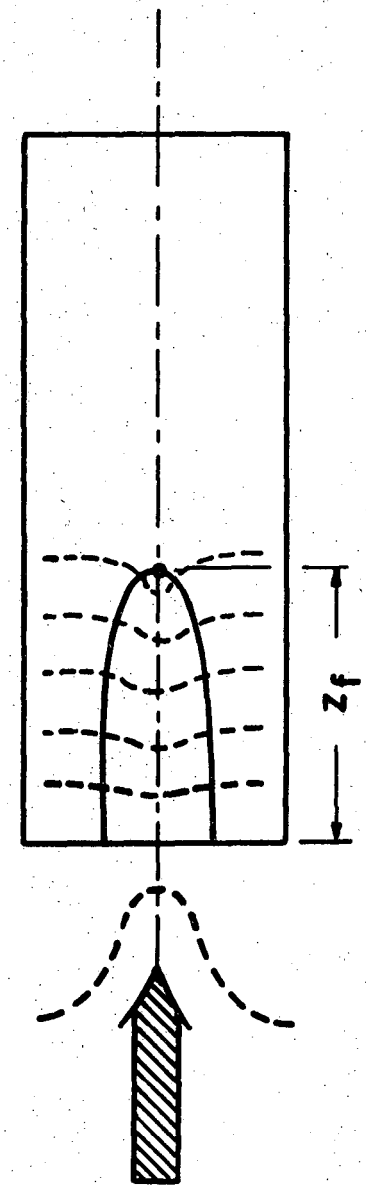

XBL 743-5891

Fig. 3

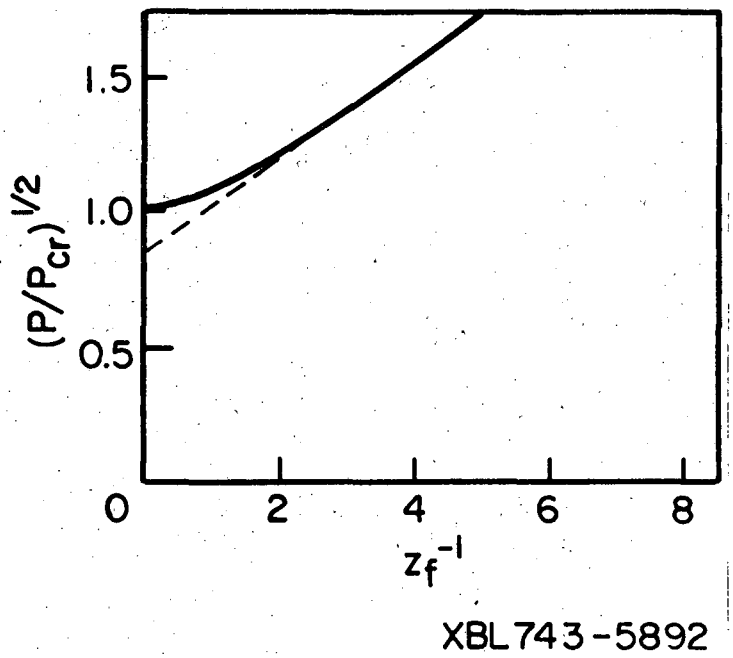

Fig. 4

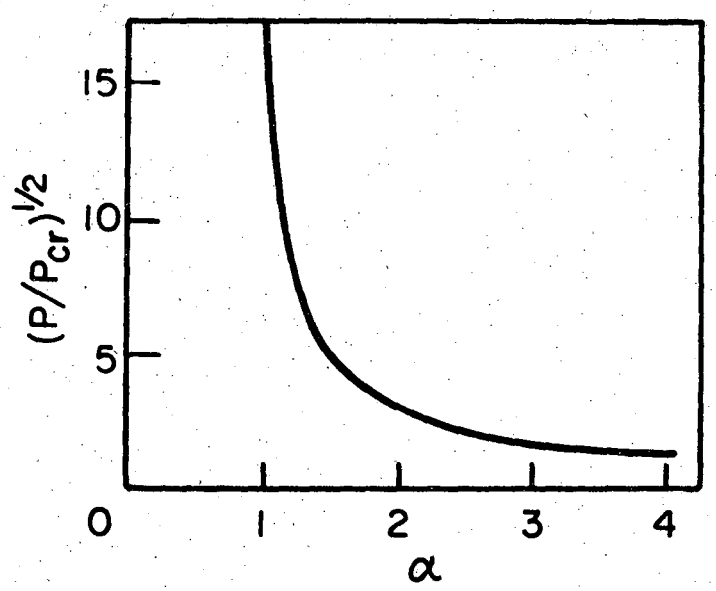

XBL743-5893

Fig. 5

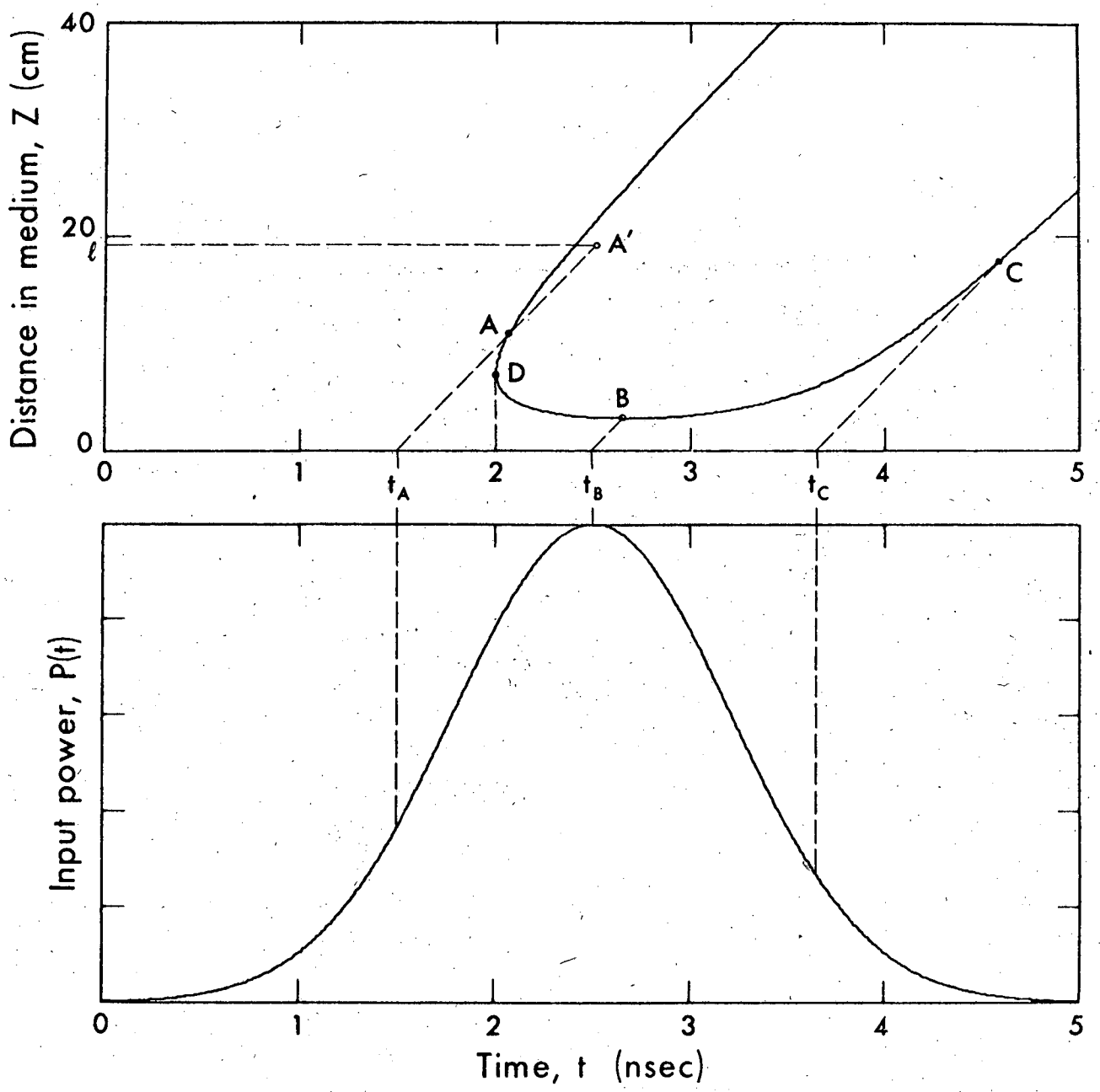

XBL 7010-6788

Fig. 6

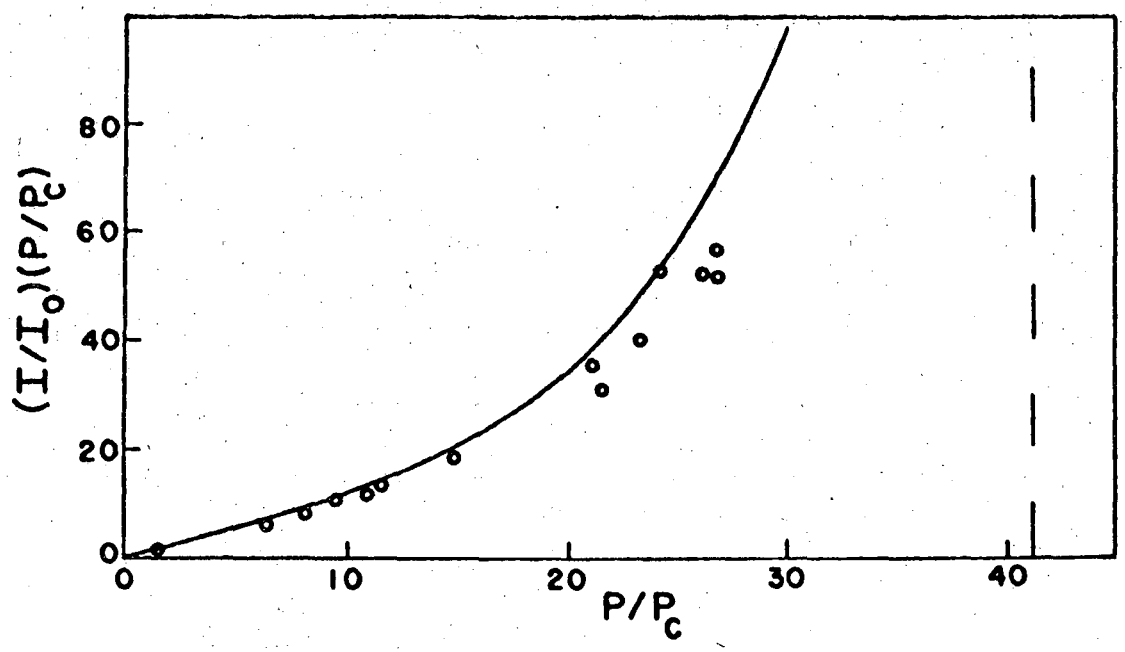

XBL 743-552

Fig. 7

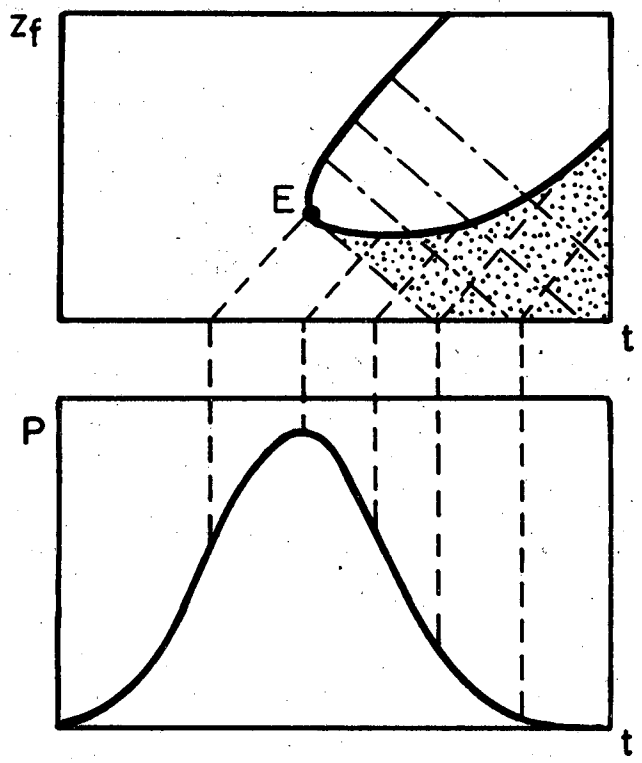

XBL743-5894

Fig. 8

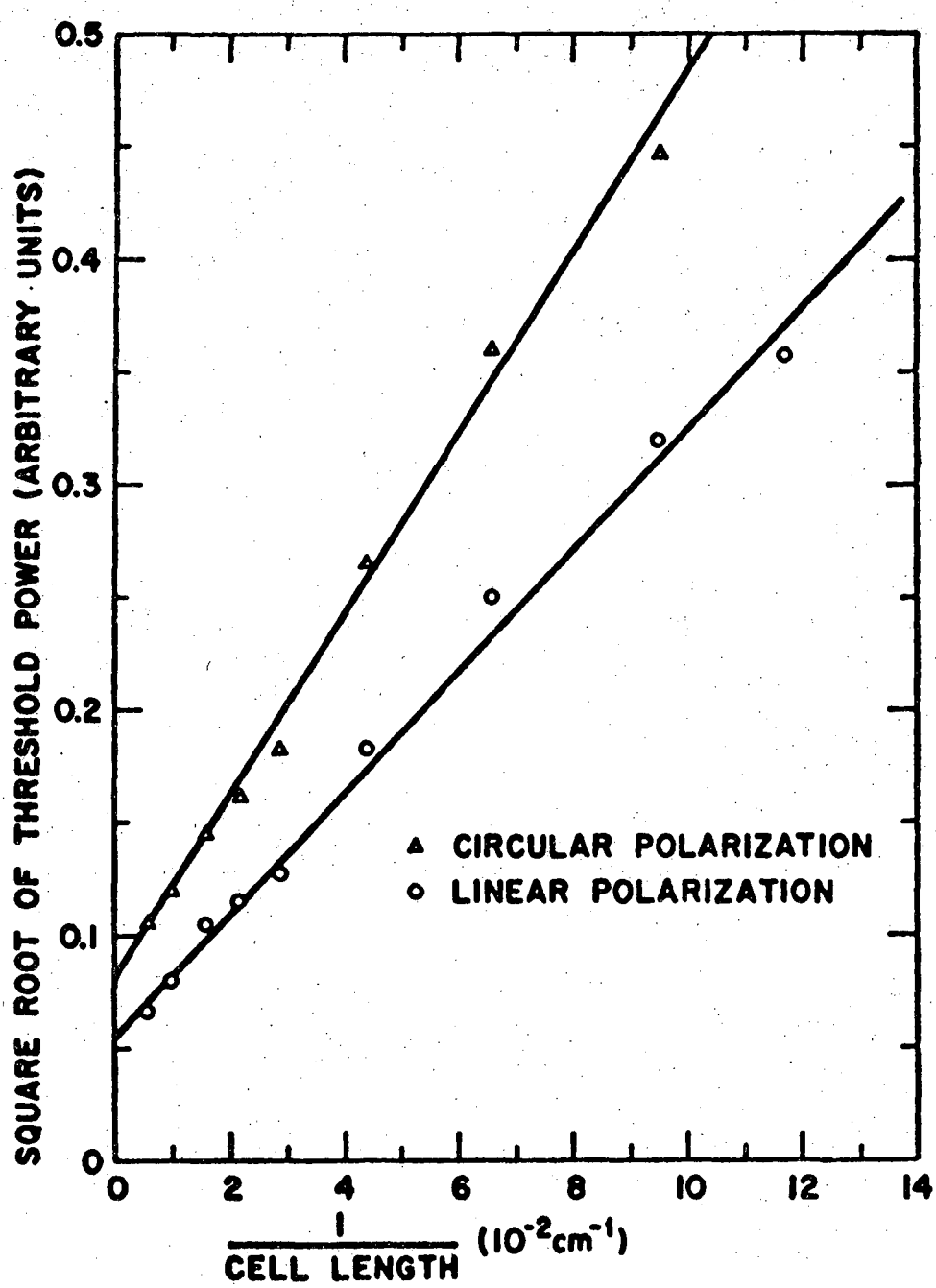

XBL 743-548

Fig. 9

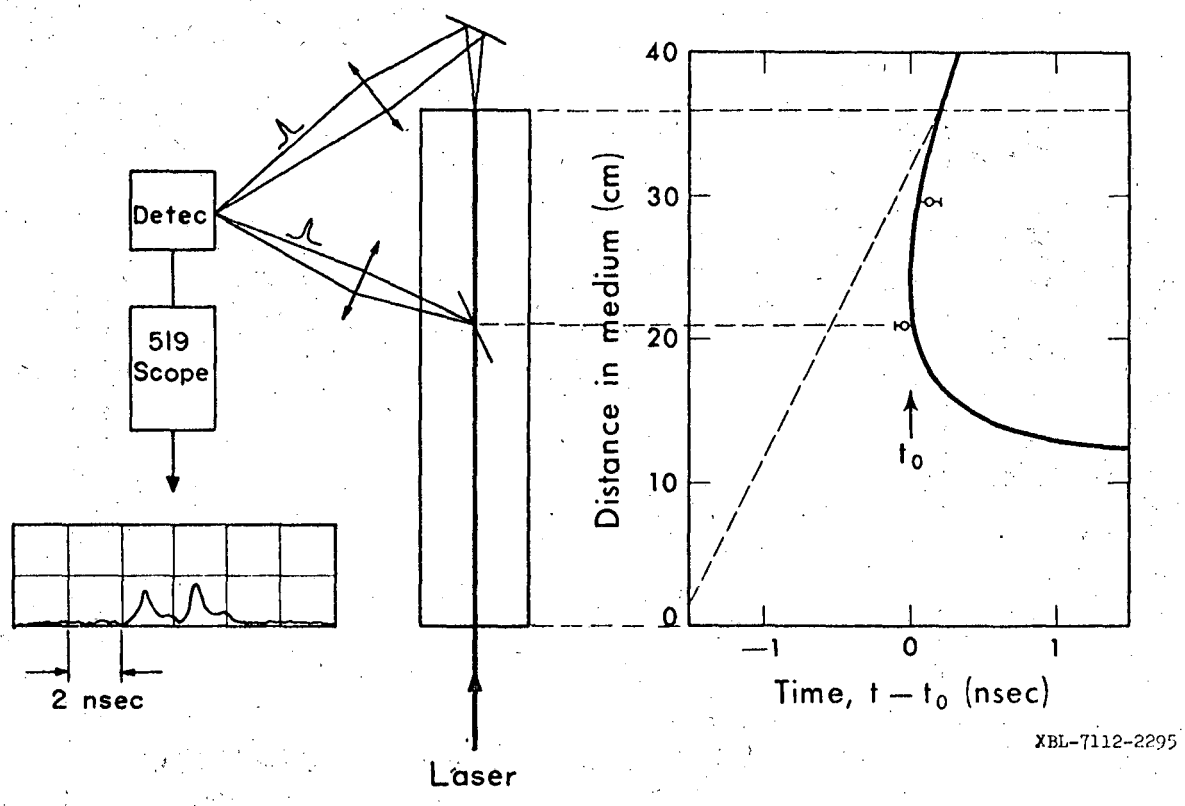
Detec
519
Scope
2 nsec
Laser
Distance in medium (cm)
40
30
20
10
0
−1
0
1
Time, t − t0 (nsec)
t0
XBL-7112-2295

Fig. 10

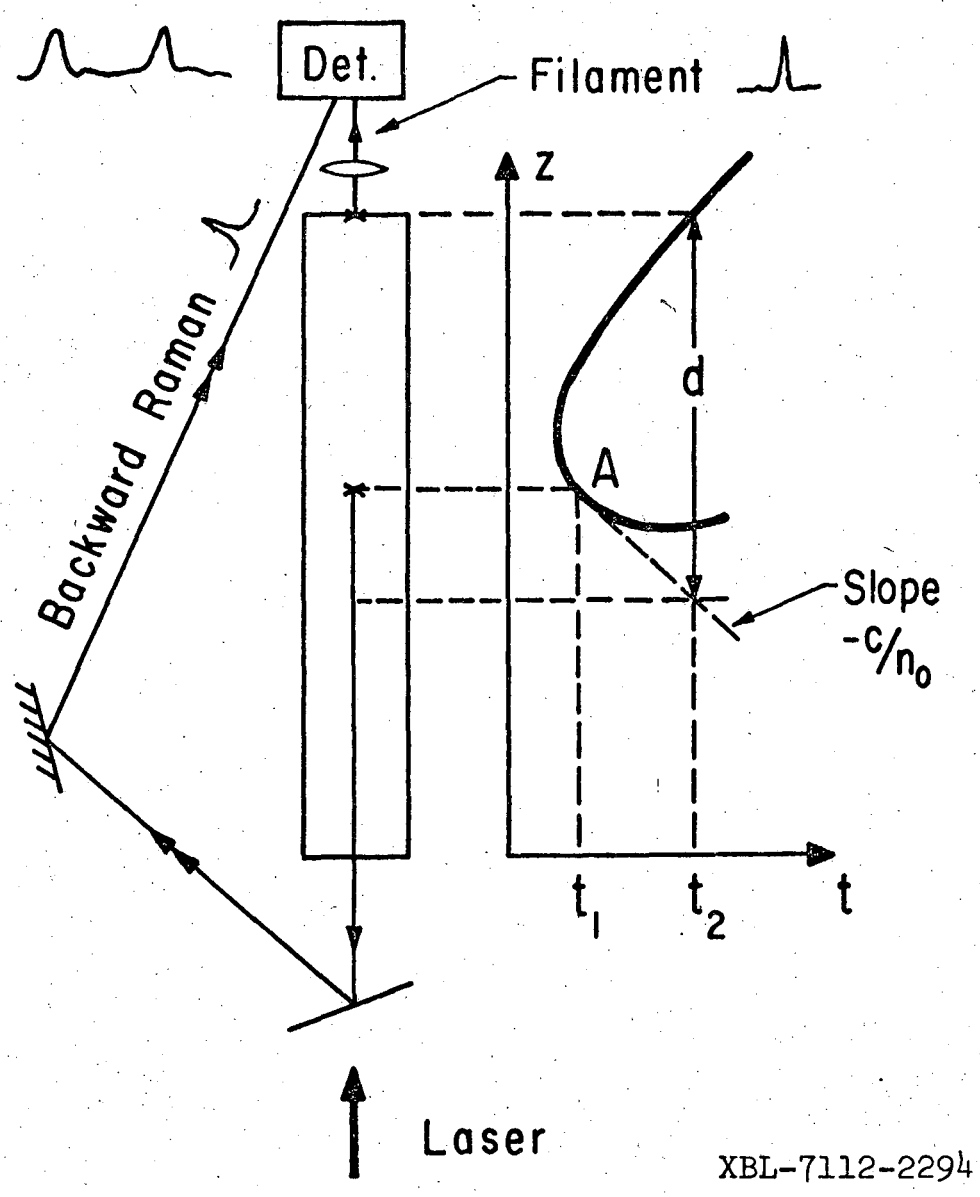
Det.
Filament
Backward Raman
z
d
A
Slope
$-c/n_0$
t_1
t_2
t
Laser
XBL-7112-2294

Fig. 11a

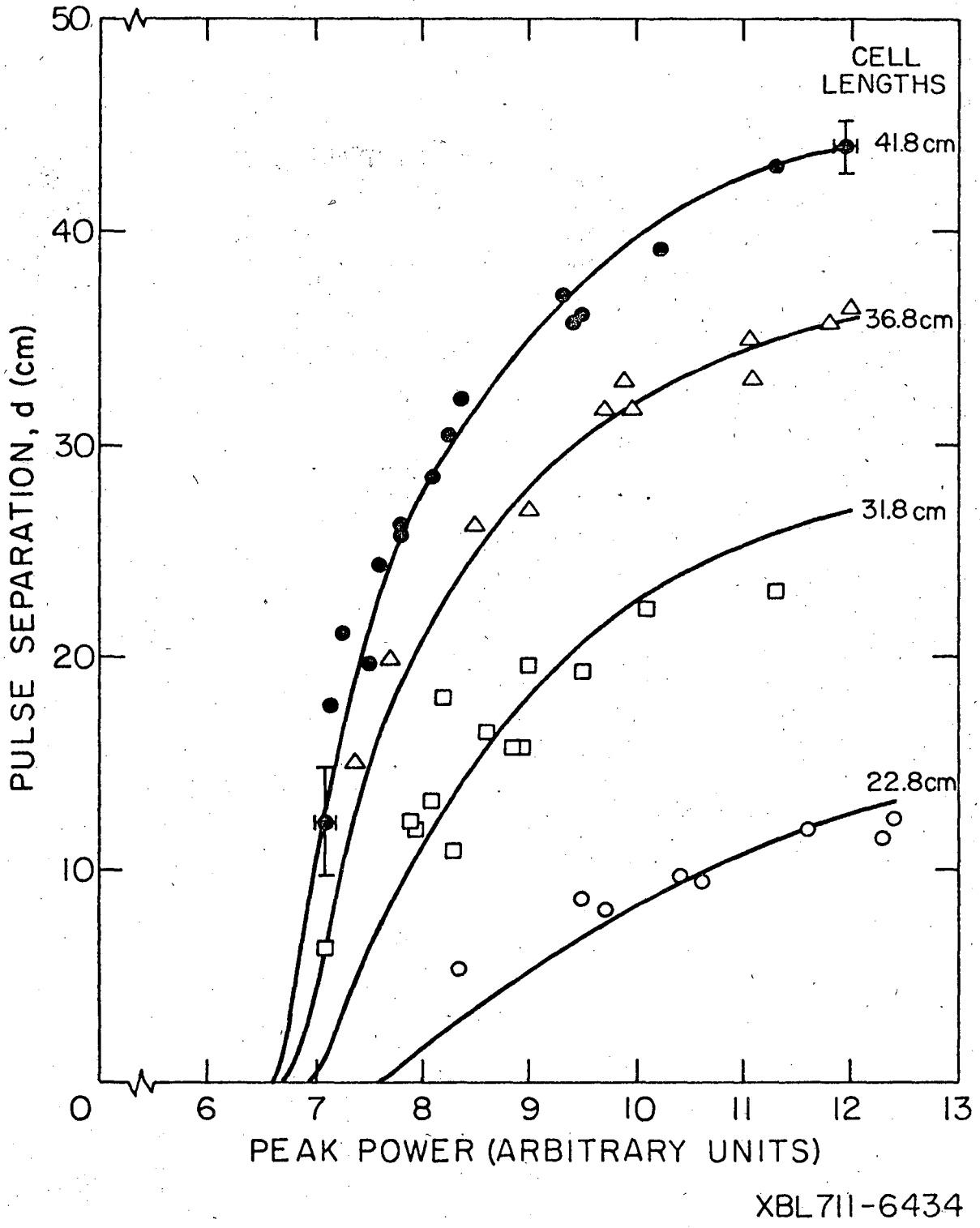
CELL LENGTHS
41.8 cm
36.8 cm
31.8 cm
22.8 cm
PULSE SEPARATION, d (cm)
PEAK POWER (ARBITRARY UNITS)
0
10
20
30
40
50
6
7
8
9
10
11
12
13
XBL711-6434

Fig. 11b

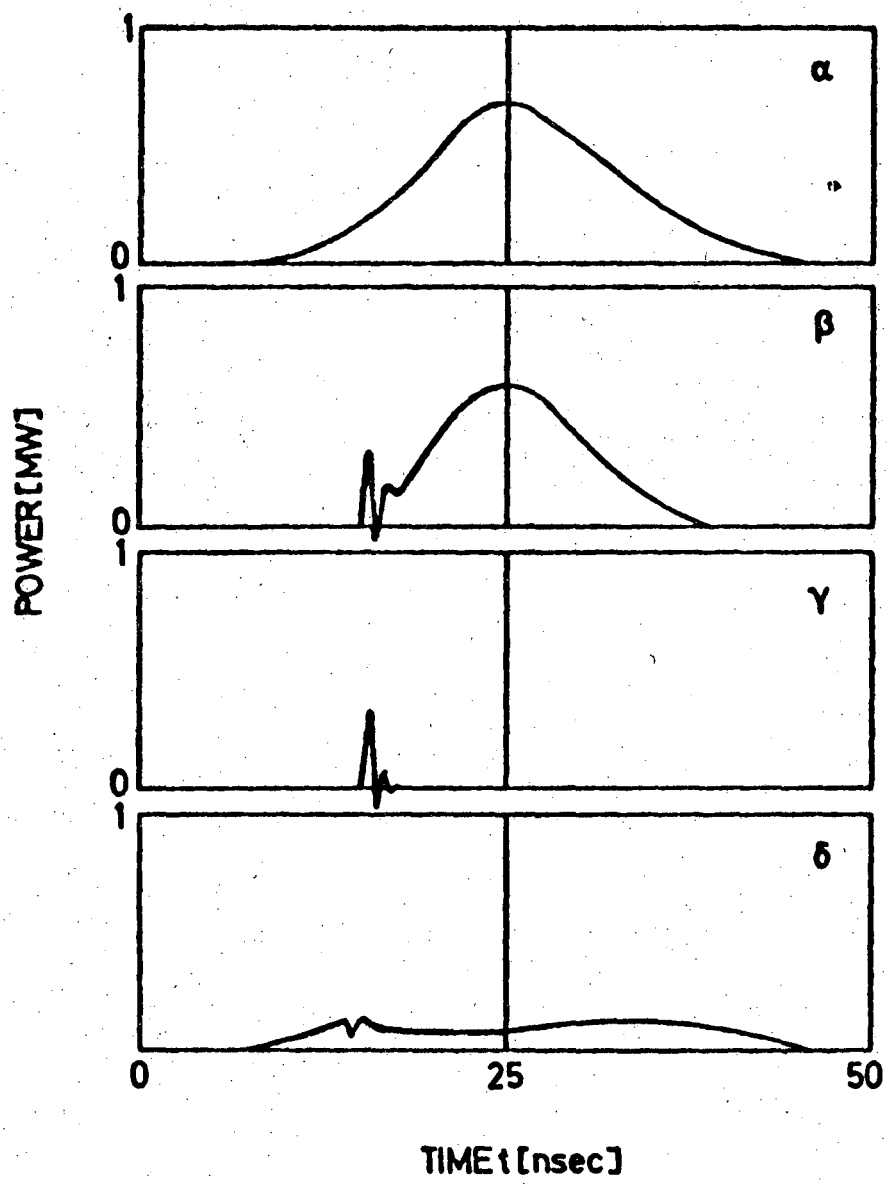

XBL 743-547

Fig. 12

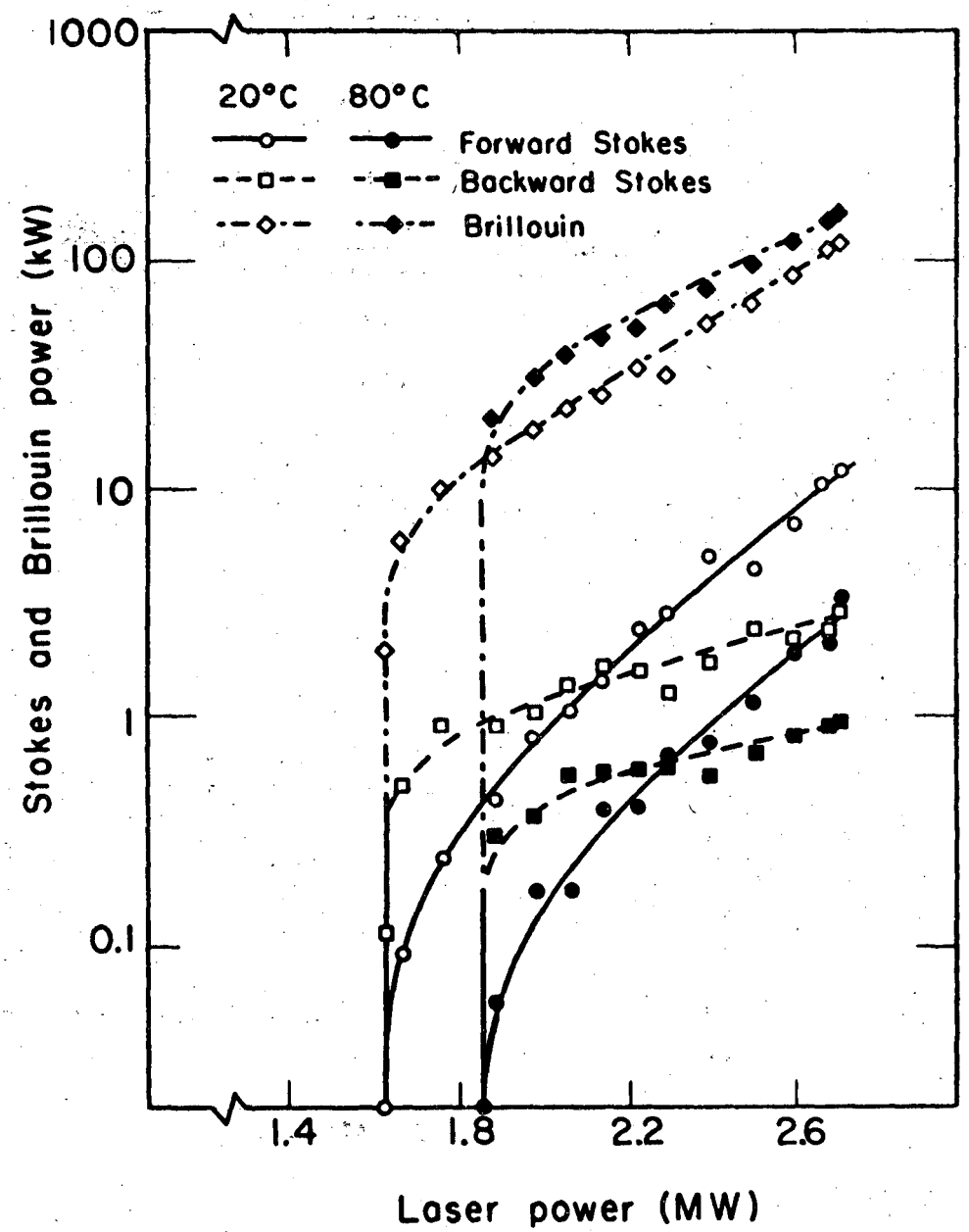

XBL 743-549

Fig. 13

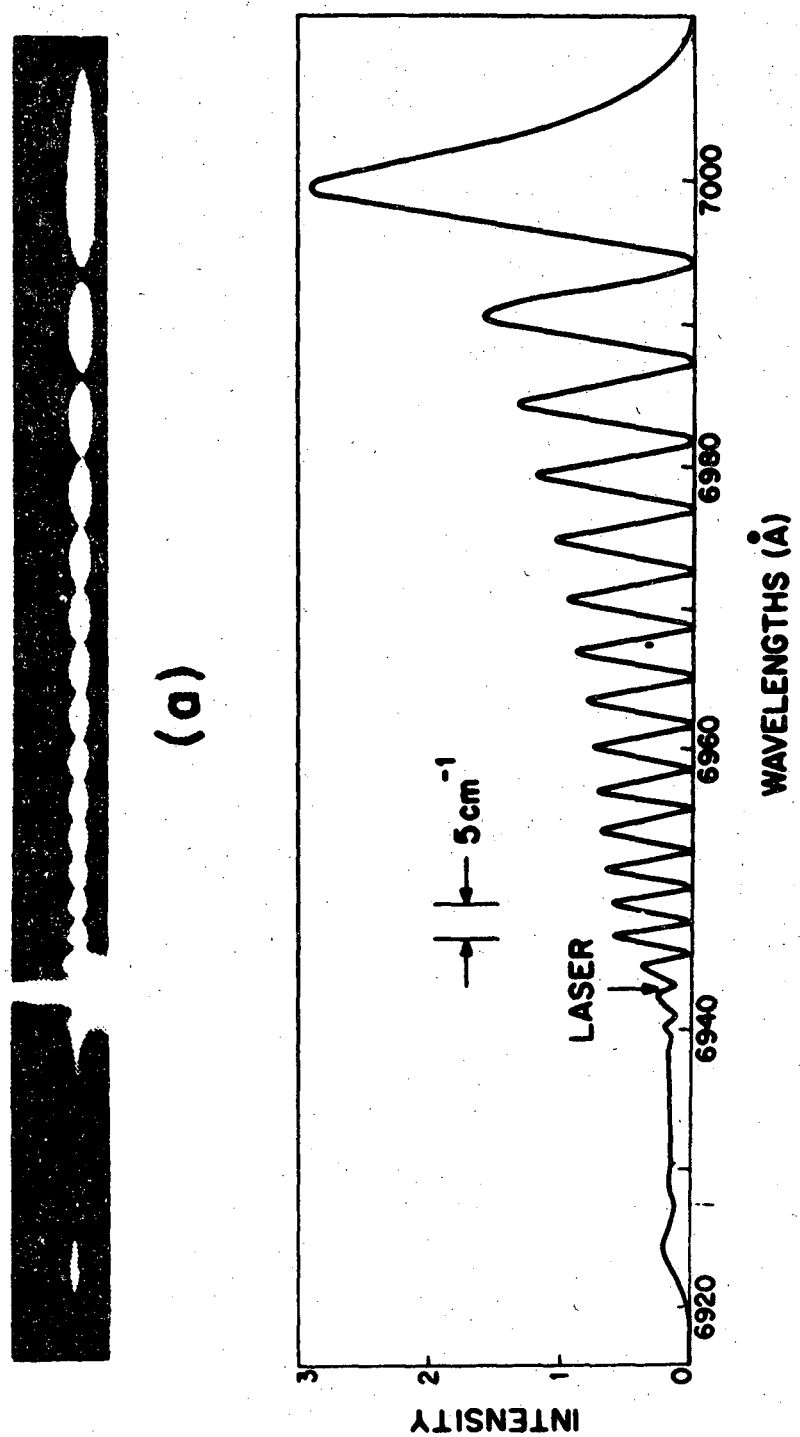
(a)
INTENSITY
3
2
1
0
6920
6940
6960
6980
7000
WAVELENGTHS (Å)
LASER
5cm⁻¹
(b)

Fig. 14

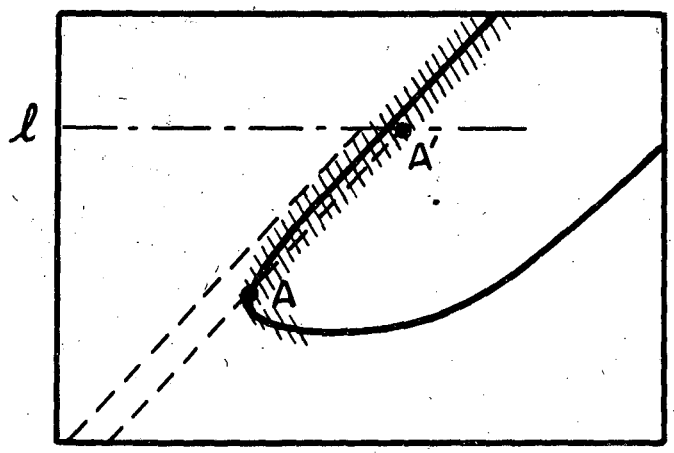

XBL743-5895

Fig. 15

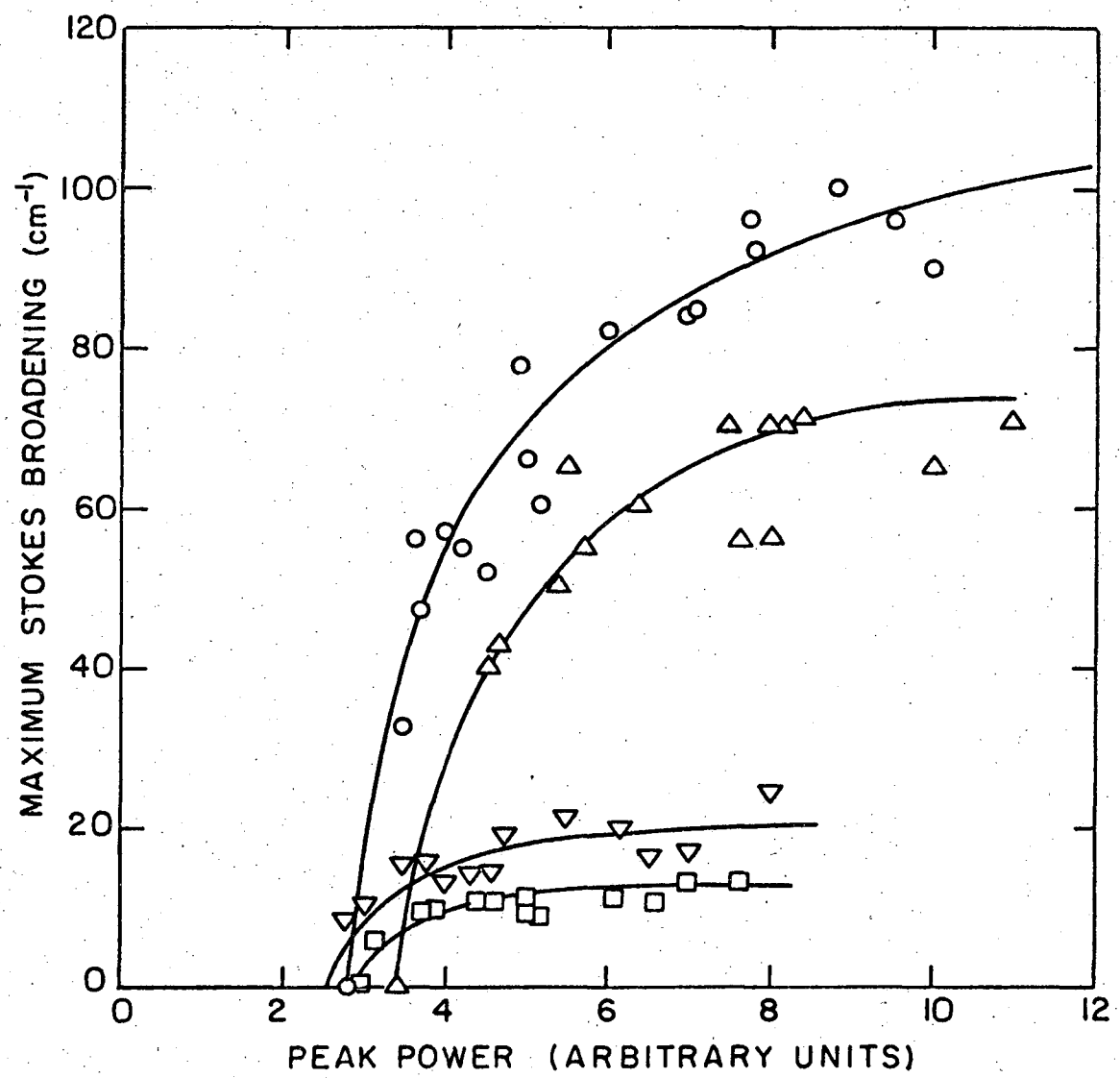

XBL721-5982

Fig. 16

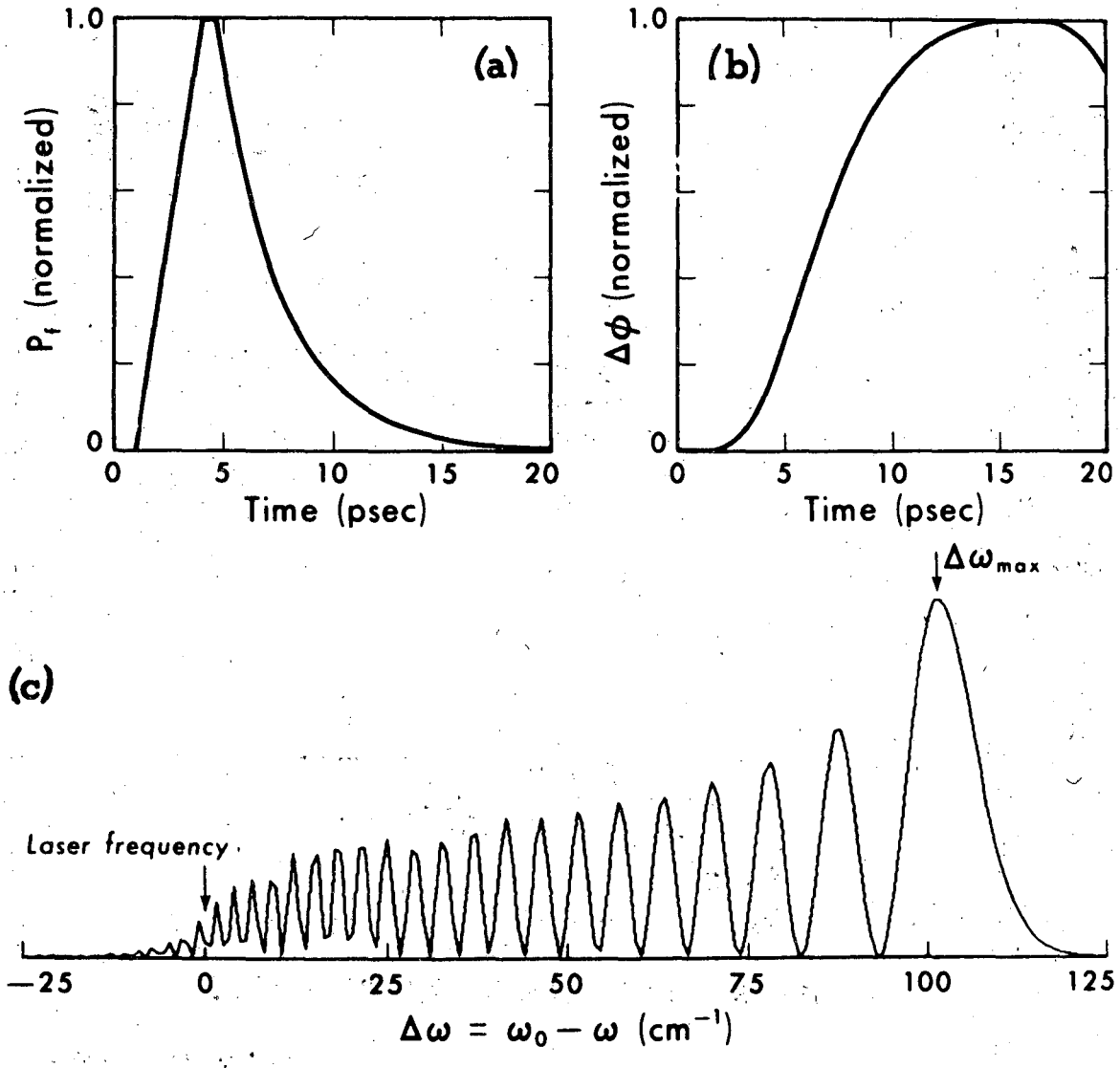

XBL 743-551

Fig. 17

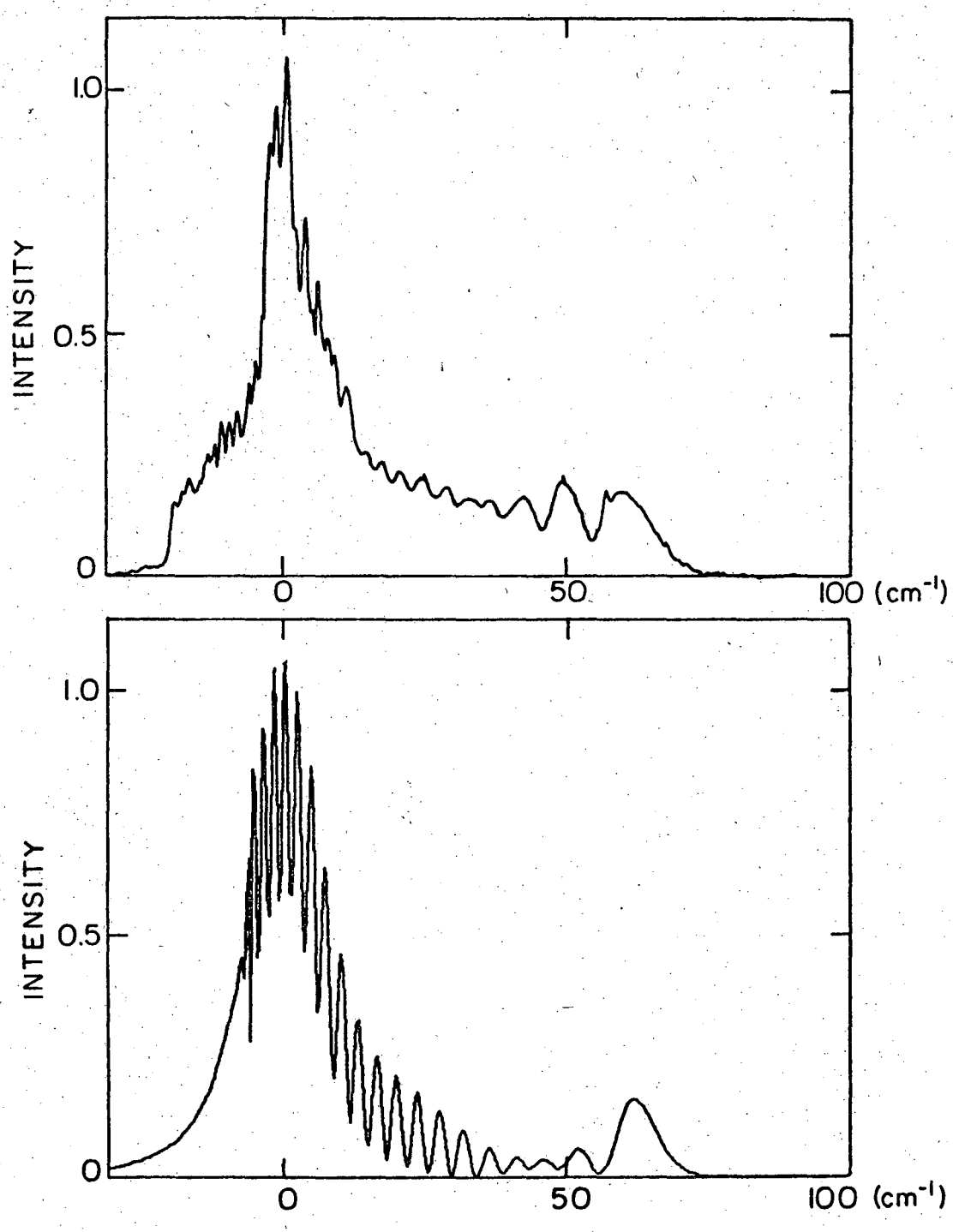

XBL 725-6248

Fig. 18

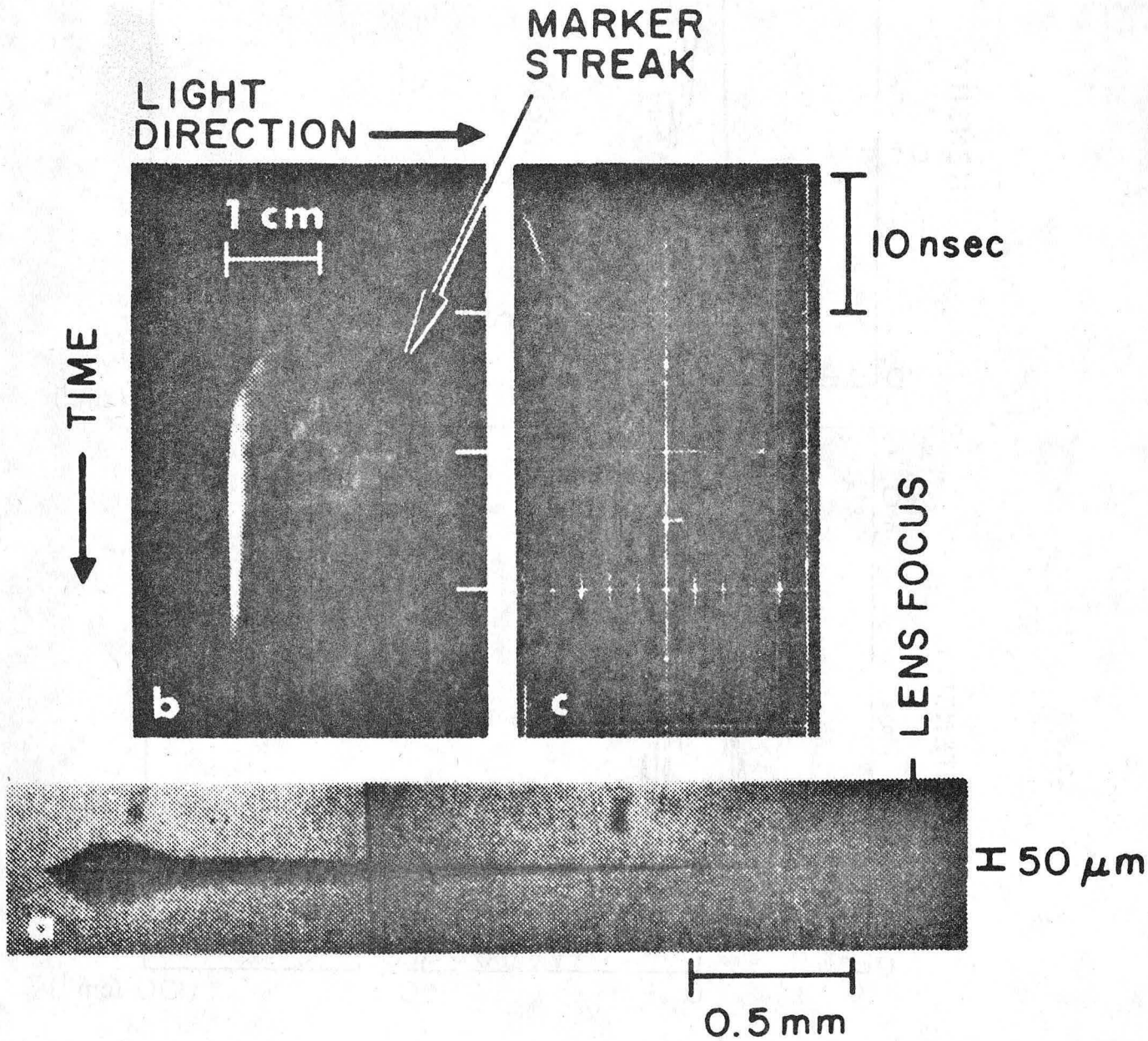
MARKER
STREAK
LIGHT
DIRECTION
1 cm
10 nsec
TIME
b
c
LENS FOCUS
50 μm
a
0.5 mm

Fig. 19

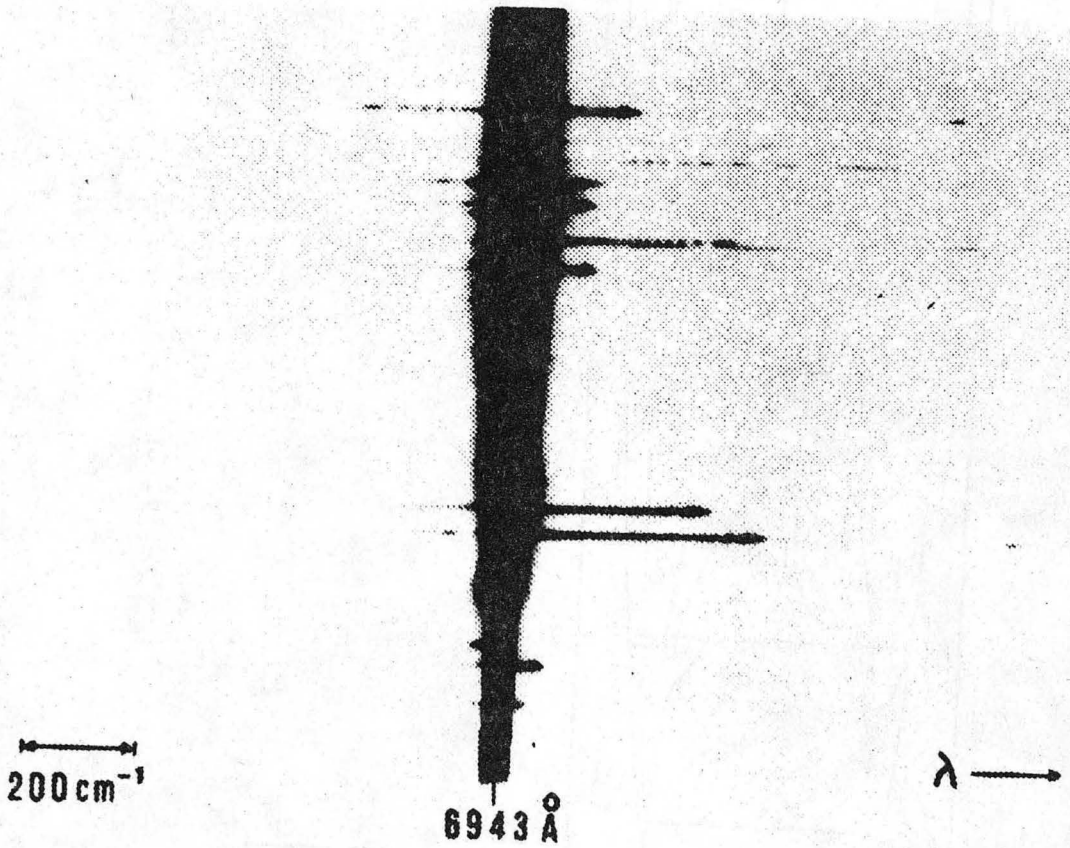

Fig. 20

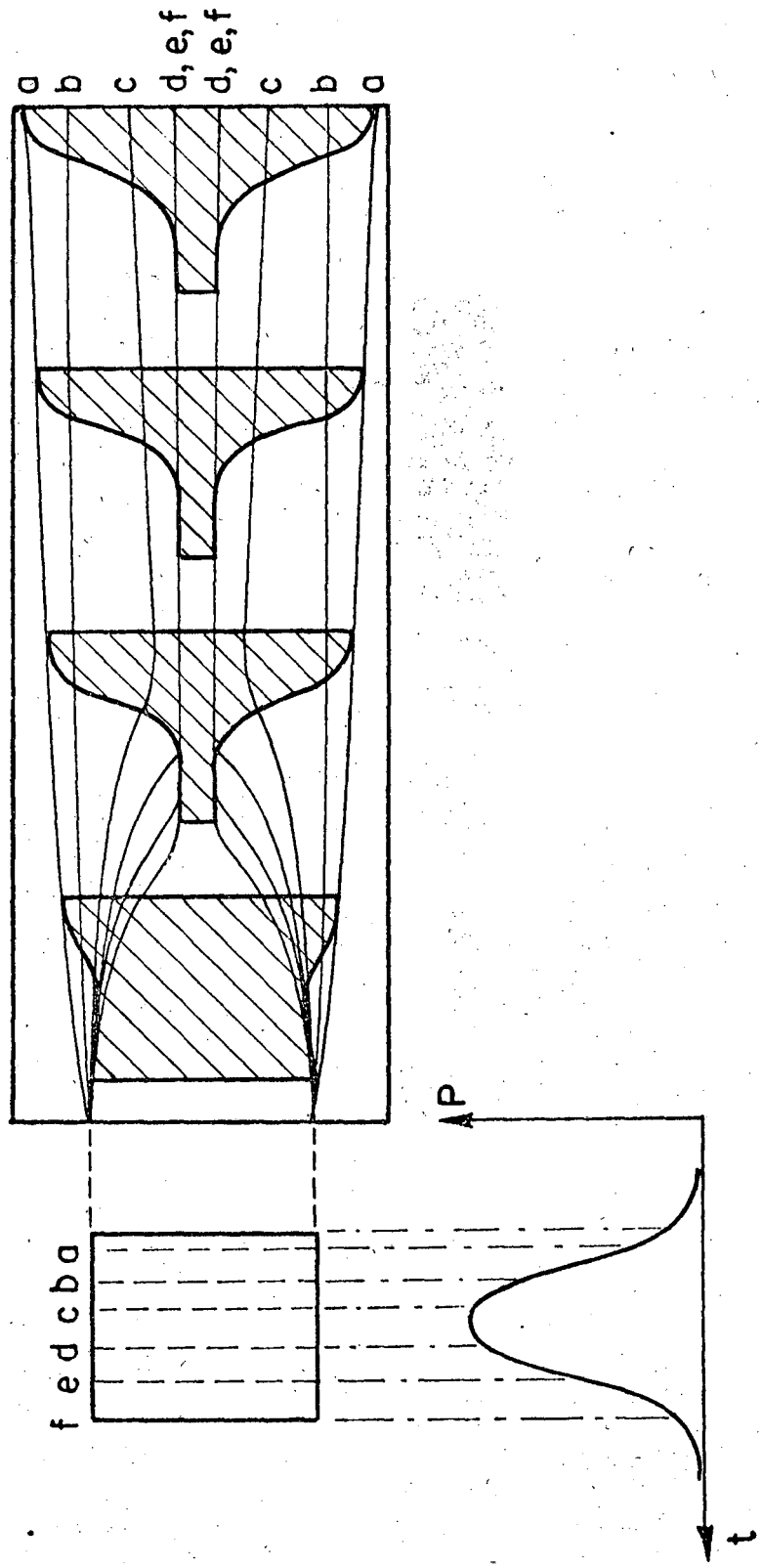

XBL7312-7163

Fig. 21

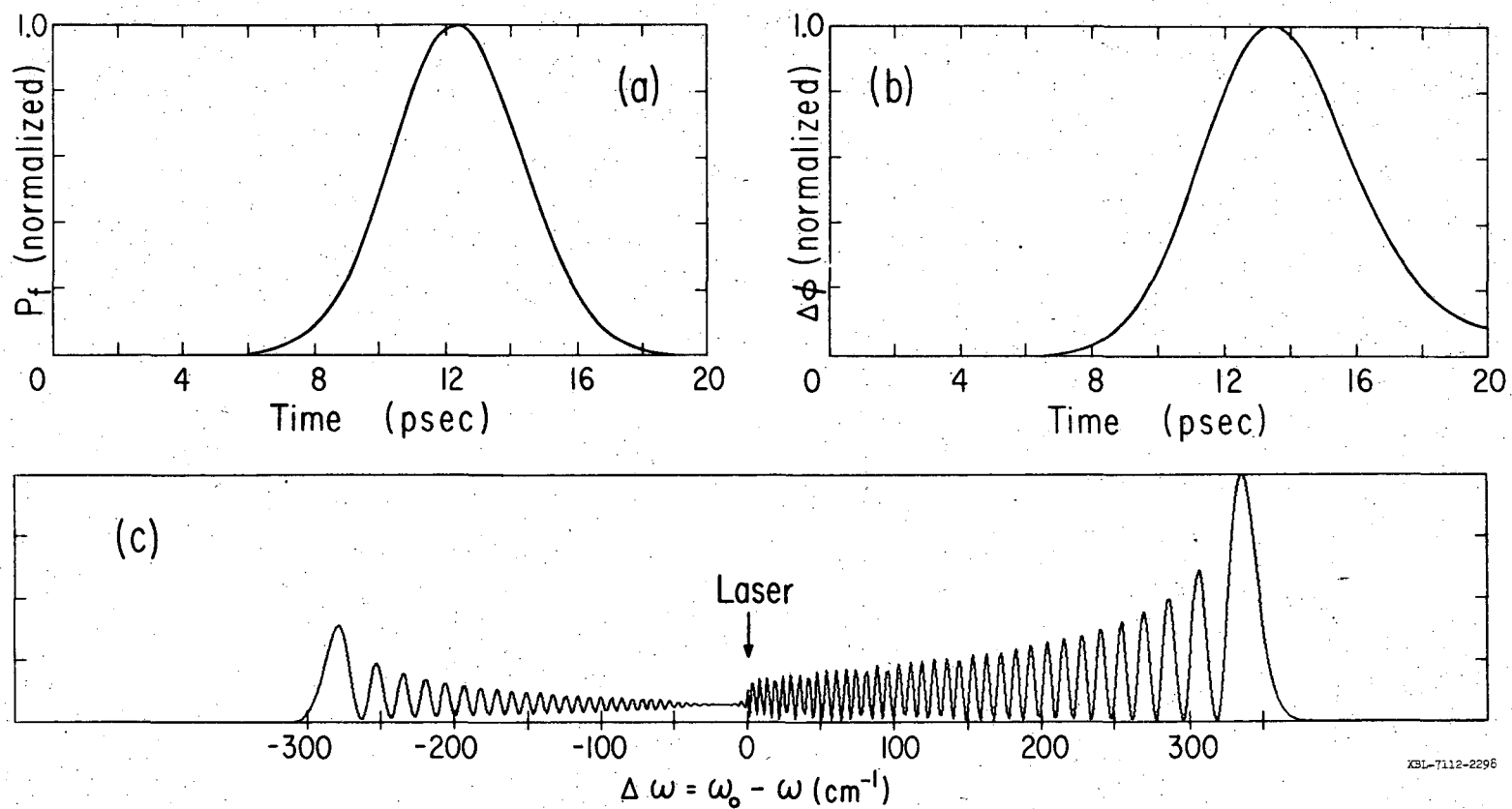
1.0
P_f (normalized)
(a)
0
4
8
12
16
20
Time (psec)
1.0
$\Delta\phi$ (normalized)
(b)
0
4
8
12
16
20
Time (psec)
(c)
Laser
-300
-200
-100
0
100
200
300
$\Delta\omega = \omega_o - \omega$ (cm^{-1})
XBL-7112-2296

Fig. 22

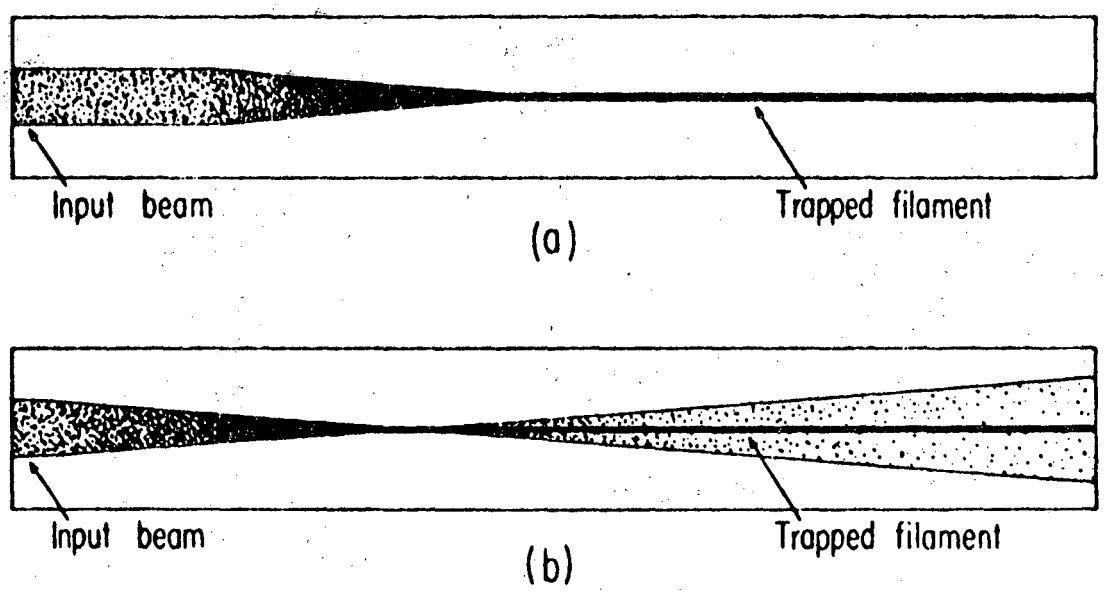

XBL 743-550

Fig. 23

LEGAL NOTICE

This report was prepared as an account of work sponsored by the United States Government. Neither the United States nor the United States Atomic Energy Commission, nor any of their employees, nor any of their contractors, subcontractors, or their employees, makes any warranty, express or implied, or assumes any legal liability or responsibility for the accuracy, completeness or usefulness of any information, apparatus, product or process disclosed, or represents that its use would not infringe privately owned rights.

TECHNICAL INFORMATION DIVISION
LAWRENCE BERKELEY LABORATORY
UNIVERSITY OF CALIFORNIA
BERKELEY, CALIFORNIA 94720